Cell Reports
Medicine

Article

Neoadjuvant fuzuloparib combined with abiraterone for localized high-risk prostate cancer (FAST-PC): A single-arm phase 2 study

Graphical abstract

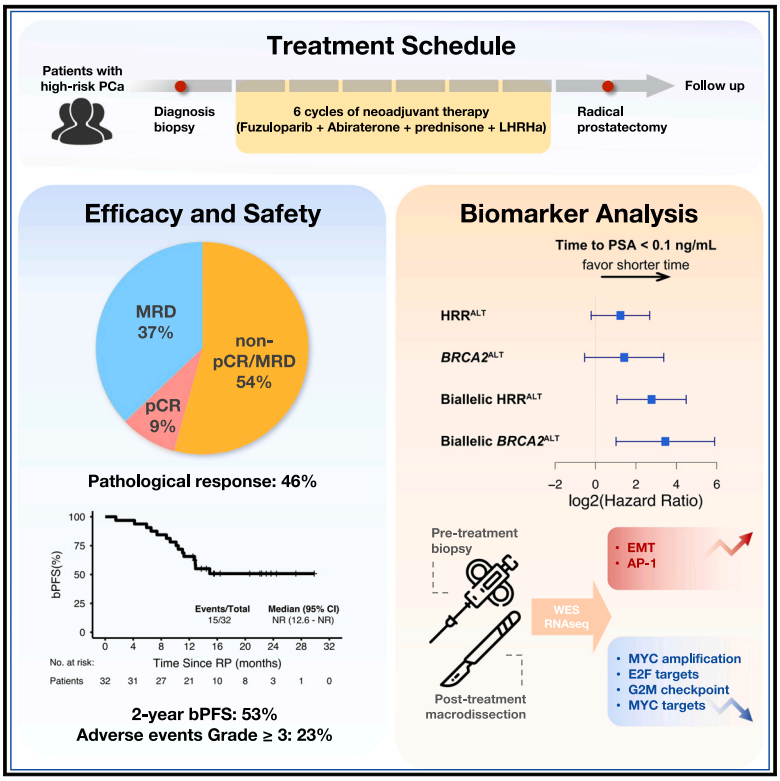

Highlights

- Neoadjuvant PARPi + ARSi shows efficacy with manageable toxicity in high-risk PCa
- Biallelic HRR/*BRCA2* alterations correlate with faster PSA decline
- Post-treatment analysis reveals MYC suppression and reduced proliferation-related pathways
- Drug-tolerant persister cells exhibit enhanced EMT and AP-1 activation

Authors

Tingwei Zhang, Beihe Wang, Yu Wei, ..., Shenglin Huang, Dingwei Ye, Yao Zhu

Correspondence

slhuang@fudan.edu.cn (S.H.), dwye.shca@gmail.com (D.Y.), zhuyao@fudan.edu.cn (Y.Z.)

In brief

Zhang et al. report a phase 2 trial evaluating neoadjuvant fuzuloparib plus abiraterone in treatment-naive men with high-risk localized prostate cancer. The combined pCR/MRD rate is 46%, with a 53% 2-year biochemical progression-free survival. The trial demonstrates feasibility, preliminary efficacy, and potential biomarkers for future studies.

Zhang et al., 2025, Cell Reports Medicine 6, 102018
March 18, 2025
https://doi.org/10.1016/j.xcrm.2025.102018

CellPress

Cell Reports Medicine

CellPress
OPEN ACCESS

Article

Neoadjuvant fuzuloparib combined with abiraterone for localized high-risk prostate cancer (FAST-PC): A single-arm phase 2 study

Tingwei Zhang,[1,2,3,10] Beihe Wang,[1,2,3,10] Yu Wei,[1,2,3] Hualei Gan,[2,4] Bangwei Fang,[1,2,3] Xiaomeng Li,[1,2,3] Junlong Wu,[1,2,3] Xiaojie Bian,[1,2,3] Jianfei Wang,[5] Stephen J. Freedland,[6,7,8] Shenglin Huang,[2,9,*] Dingwei Ye,[1,2,3,*] and Yao Zhu[1,2,3,11,*]

[1]Department of Urology, Fudan University Shanghai Cancer Center, Shanghai, China
[2]Department of Oncology, Shanghai Medical College, Fudan University, Shanghai, China
[3]Shanghai Genitourinary Cancer Institute, Shanghai, China
[4]Department of Pathology, Fudan University Shanghai Cancer Center, Shanghai, China
[5]Jiangsu Hengrui Pharmaceuticals Co., Ltd, Shanghai, China
[6]Samuel Oschin Comprehensive Cancer Institute, Cedars-Sinai Medical Center, Los Angeles, CA, USA
[7]Department of Urology, Cedars-Sinai Medical Center, Los Angeles, CA, USA
[8]Section of Urology, Durham VA Medical Center, Durham, NC, USA
[9]Department of Medical Oncology, Fudan University Shanghai Cancer Center, and Shanghai Key Laboratory of Medical Epigenetics, International Co-laboratory of Medical Epigenetics and Metabolism, Institutes of Biomedical Sciences, Fudan University, Shanghai, China
[10]These authors contributed equally
[11]Lead contact
*Correspondence: slhuang@fudan.edu.cn (S.H.), dwye.shca@gmail.com (D.Y.), zhuyao@fudan.edu.cn (Y.Z.)
https://doi.org/10.1016/j.xcrm.2025.102018

SUMMARY

Preclinical studies suggest synergistic effects between androgen receptor inhibitors and poly(adenosine diphosphate-ribose) polymerase (PARP) inhibitors. This phase 2 trial (NCT05223582) evaluates neoadjuvant fuzuloparib plus abiraterone in 35 treatment-naive men with localized high-risk prostate cancer. Patients receive six cycles of therapy followed by radical prostatectomy. Primary endpoints are pathological complete response (pCR) and minimal residual disease (MRD, $\leq$5 mm). The combined pCR/MRD rate is 46% (95% confidence interval [CI]: 29%–63%), with a 53% 2-year biochemical progression-free survival rate. Grade $\geq$3 adverse events occur in 23% of patients. Biallelic homologous recombination repair/*BRCA2* alterations correlate with faster prostate-specific antigen decline. Post-treatment genomic analyses reveal reduced MYC amplification and proliferation markers, alongside activated epithelial-mesenchymal transition/activator protein 1 (AP-1) pathways. The trial meets its primary endpoint, demonstrating feasibility and preliminary efficacy, while exploratory biomarkers may guide future studies.

INTRODUCTION

Radical prostatectomy (RP) is a standard therapeutic approach for patients with clinically localized prostate cancer (PCa). However, individuals presenting with high-risk features, such as serum prostate-specific antigen (PSA) levels exceeding 20 ng/mL, advanced stage ($\geq$cT3), and high-grade tumors (grade group 4 or 5), face an elevated risk of biochemical recurrence and metastasis post RP.[1] These patients, particularly those with nodal involvement (cN1), are most likely to benefit from intensified treatment strategies,[2] which has led to the integration of multimodal approaches to optimize disease control.[3,4]

Neoadjuvant conventional androgen deprivation therapy (ADT) has been shown to reduce positive surgical margins and extraprostatic extension but does not significantly improve survival outcomes.[5] Over the past decade, intensified androgen receptor signaling inhibitors (ARSis), including abiraterone, enzalutamide, and apalutamide, have been explored as preoperative treatments for localized PCa. Favorable pathological responses, such as pathological complete response (pCR, defined as the absence of morphologically identifiable carcinoma in the RP specimen), and minimal residual disease (MRD, defined as the maximum diameter of residual tumor $\leq$5 mm) have been observed in 6.4%–30% of cases (Table S1).

Poly(adenosine diphosphate-ribose) polymerase inhibitors (PARPis), such as olaparib, talazoparib, and niraparib, have received approval from the US Food and Drug Administration for use in combination with ARSis as first-line treatment for patients with metastatic castration-resistant prostate cancer (mCRPC) harboring homologous recombination repair (HRR) gene defects (e.g., talazoparib plus enzalutamide) or *BRCA* mutations (e.g., olaparib plus abiraterone, niraparib plus abiraterone). However, the majority of research on ARSi and PARPi combination therapy has concentrated on the mCRPC stage, with limited studies addressing early-stage PCa. The prevalence of HRR mutations in localized PCa ranges from 8% to 12% in

Table 1. Baseline characteristics

Characteristics	Patients (*N* = 35)
Age	
Median (range), years	72 (52–82)
<60, *n* (%)	4 (11.4%)
60–70, *n* (%)	7 (20.0%)
≥70, *n* (%)	24 (68.6%)
ECOG PS, *n* (%)	
0	31 (88.6%)
1	4 (11.4%)
Clinical T stage, *N* (%)	
T2	16 (45.7%)
T3a	4 (11.4%)
T3b	5 (14.3%)
T4	10 (28.6%)
Clinical N stage, *N* (%)	
N0	25 (71.4%)
N1	10 (28.6%)
Gleason score, *N* (%)	
7 (3 + 4)[a]	1 (2.9%)
7 (4 + 3)	3 (8.6%)
8	12 (34.3%)
9	16 (45.7%)
10	3 (8.6%)
PSA (ng/mL)	
Median (range), ng/mL	46.9 (3.41–470)
<20, *N* (%)	5 (14.3%)
20–100, *N* (%)	20 (57.1%)
≥100, *N* (%)	10 (28.6%)
NCCN risk group, *N* (%)	
High risk	3 (8.6%)
Very high risk	32 (91.4%)
STAMPEDE high-risk criteria[b]	
Yes	34 (97.1%)
No	1 (2.9%)

ECOG PS, Eastern Cooperative Oncology Group performance status; PSA, prostate-specific antigen.

[a]The patient was diagnosed in 2016 and subsequently underwent active surveillance. The Gleason score was assessed based on the 2016 biopsy specimens.

[b]Defined as node positive or, if node negative, having at least two of the following: tumor stage T3 or T4, Gleason score of 8–10, and PSA ≥ 40 ng/mL.[16]

predominantly Caucasian cohorts.[6,7] Given the association of *BRCA1/2* mutations with more advanced disease,[8] their prevalence is likely higher among high-risk patients.

Recent advancements in understanding the biology of PCa suggest that combining PARPi and ARSi may exert synergistic effects.[9] Evidence indicates that this combination significantly prolongs radiographic progression-free survival in patients with mCRPC, irrespective of genomic alterations, though the extent of benefit for individuals without *BRCA* mutations remains debated.[10–12] In hormone-naive settings, the infrequent occurrence of androgen receptor (AR) pathway alterations implies that ARSis may induce a state of "BRCAness," enhancing tumor susceptibility to PARPis.[9,13]

Fuzuloparib, a PARPi,[14] has been approved in China for the treatment of high-grade, platinum-sensitive, recurrent ovarian cancer based on the FZOCUS-2 trial.[15] A double-blind, randomized phase 3 trial (NCT04691804) is currently investigating fuzuloparib combined with abiraterone versus placebo with abiraterone as first-line treatment in unselected patients with mCRPC. The FAST-PC trial was conducted to assess the efficacy and safety of fuzuloparib combined with abiraterone as neoadjuvant therapy in patients with localized high-risk PCa. Additionally, this study aimed to identify potential predictive biomarkers of treatment efficacy and to explore the genomic characteristics of drug-tolerant persister cells, thereby providing comprehensive evidence to guide and optimize future clinical trials.

RESULTS

Patients

Between June 23, 2021, and November 4, 2022, 35 eligible patients were enrolled and received the study treatment. Three patients discontinued the assigned neoadjuvant therapy, and two did not undergo RP, resulting in 30 patients included in the per-protocol (PP) population (Figure S1). Baseline characteristics are summarized in Table 1. The median age was 72 years, with 19 patients (54%) presenting with clinical T stage ≥ T3 and 10 patients (29%) having clinical lymph node metastasis. 19 patients (54%) were classified as International Society of Urological Pathology grade group 5 (16 with Gleason sum 9; 3 with Gleason sum 10). Furthermore, 32 patients (91%) were categorized as having National Comprehensive Cancer Network (NCCN) very high-risk disease,[3] and 34 patients (97%) met the high-risk criteria of the STAMPEDE trial.[16]

Efficacy

In the intention-to-treat (ITT) population, three patients (9%, 95% confidence interval [CI]: 2%–23%) achieved pCR, and 13 patients (37%, 95% CI: 22%–55%) achieved MRD. The study met its primary endpoint with a pathological response rate of 46% (95% CI: 29%–63%) in the ITT population (Figure 1A). The PP population exhibited similar results, with a pCR rate of 10% (95% CI: 2%–27%) and an MRD rate of 40% (95% CI: 23%–59%) (Figure 1A). Consistent pathological response rates were observed across all subgroups, except for patients with clinical T4 stage (20%, 95% CI: 3%–56%) (Figure 1B). Representative pathological responses after neoadjuvant treatment are shown in Figure 1C. Of the 33 patients who underwent RP, only one (3%) had positive surgical margins.

Among the 30 patients who underwent RP with available baseline and pre-RP MRI data, 87% were staged as cT2 pre-RP compared to 47% at baseline. Radiological assessments indicated lower rates of lymph node involvement at RP compared to baseline (13% vs. 33%, respectively) (Figures 2A and 2B). Representative radiological responses, including a patient (P34) with a biallelic *BRCA2* mutation, are depicted in Figure 2C.

A

	Intention-to-treat population (n=35)	Per-protocol population (n=30)
Pathological response	16 (45.7%)	15 (50.0%)
pCR	3 (8.6%)	3 (10.0%)
MRD	13 (37.1%)	12 (40.0%)

B

	No. of responders / No. of pts	Pathological response rate (95%CI)
Intention-to-treat population	16/35	45.7 (28.8–63.4)
Tumor size		
cT2	9/16	56.3 (29.9–80.3)
cT3	5/9	55.6 (21.2–86.3)
cT4	2/10	20.0 (2.5–55.6)
Nodal status		
cN0	13/25	52.0 (31.3–72.2)
cN1	3/10	30.0 (6.7–65.2)
Grade group		
2-3	2/4	50.0 (6.8–93.2)
4	6/12	50.0 (21.1–78.9)
5	8/19	42.1 (20.3–66.5)
PSA (ng/mL)		
<20	2/5	40.0 (5.3–85.3)
20-100	7/20	35.0 (15.4–59.2)
>100	7/10	70.0 (34.8–93.3)

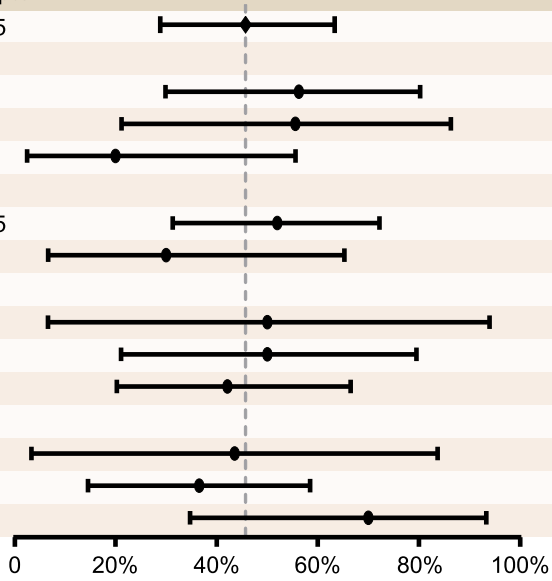

C

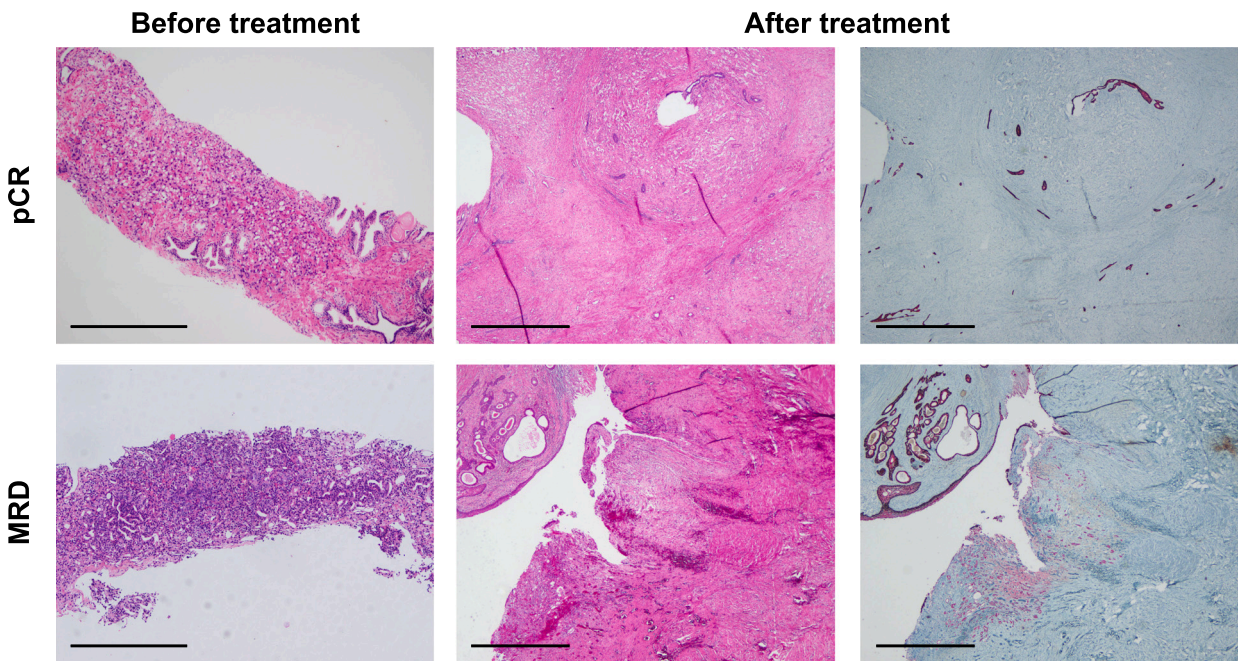

(legend on next page)

The patients presented with a median baseline PSA level of 46.9 ng/mL (interquartile range [IQR]: 30.1–114.0 ng/mL). Following three and six cycles of neoadjuvant therapy, median PSA reductions of 99.3% and 99.9% were achieved, respectively, resulting in median PSA levels of 0.21 (IQR: 0.12–0.52 ng/mL) and 0.06 ng/mL (IQR: 0.02–0.23 ng/mL) (Figure 2D). Postoperatively, eight patients were advised to receive adjuvant therapy due to the presence of ypT3/4 or ypN1 disease. Four patients opted for surveillance instead of adjuvant therapy, while the remaining four patients underwent continuous adjuvant medical castration. Adjuvant radiotherapy was not administered due to COVID-19 restrictions. Following the COVID-19 period, these patients subsequently received salvage radiotherapy.

One patient demonstrated radiological progression characterized by extensive tumor invasion and involvement of multiple pelvic lymph nodes following six treatment cycles. A rebiopsy indicated an active tumor with DNA mismatch repair (dMMR) deficiency. The patient achieved disease remission after transitioning to immunotherapy (tislelizumab) and subsequently underwent RP, with postoperative pathology confirming a pCR (which was not included in the calculation of pCR rates in our study).

Follow-up

The swimmer plot (Figure 3A) delineates the duration of treatment and outcomes throughout the study period. As of the data cutoff on May 31, 2024, with a median follow-up of 21.7 months from enrollment (IQR, 20.7 to 27.4 months) and a median post-RP follow-up of 16.2 months (IQR, 14.1 to 21.9 months), the 2-year biochemical progression-free survival (bPFS) was 53%, and the 2-year metastasis-free survival (MFS) was 94% (Figures 3B and 3C). During this period, one patient succumbed, and 14 patients experienced biochemical recurrence (BCR). There was no significant difference in bPFS between patients who achieved pCR/MRD and those who did not (p = 0.45, Figure S2A), which may be influenced by the fact that four of the 16 non-pCR/MRD patients received continuous adjuvant medical castration. The recurrence sites of the 14 BCR patients are depicted in Figure 3D, with the majority of recurrences localized to the prostate bed (n = 6) and pelvic lymph nodes (n = 4) (Figure 3D). These patients were managed with salvage radiation plus medical castration. One patient who developed supraclavicular lymph node metastasis was treated with medical castration plus abiraterone. All recurrent patients exhibited a favorable PSA response (>90%).

To account for the potential impact of continuous adjuvant medical castration on bPFS and MFS post RP, we analyzed patients who were untreated post RP and had recovered testosterone levels (>150 ng/dL). The median bPFS duration since testosterone recovery was 5.3 months (95% CI, 5.3 to not reached [NR] months, Figure 3E). Additionally, patients who achieved pCR/MRD appeared to have a longer bPFS since testosterone recovery, although this difference was not statistically significant (11.6 months [95% CI, 4.6 to NR months] vs. 4.4 months [95% CI, 3.3 to NR months], p = 0.24, Figure S2B).

Safety

All 35 patients received at least one dose of the study treatment. Among them, 33 patients (94%) experienced at least one treatment-related adverse event (TRAE) (Figure 4A). The most common TRAEs were anemia (66%, n = 23), increased alanine aminotransferase (26%, n = 9), and decreased platelet count (20%, n = 7). Grade 3 TRAEs were reported in five patients (14%), which included anemia (6%, n = 2), abnormal hepatic function (6%, n = 2), increased alanine aminotransferase (3%, n = 1), hypokalemia (3%, n = 1), and increased aspartate aminotransferase (3%, n = 1). Patients with grade 2/3 anemia generally resolved to grade 1 within 1 month following a dose reduction of fuzuloparib, except for one patient who withdrew consent (Figure 4B). No transfusions were required. One patient developed grade 4 drug-induced liver injury and recovered after discontinuing the medication. Another patient succumbed to myelodysplastic syndrome (MDS), diagnosed 7 months post RP, which led to death 3 months later. Whole-exome sequencing (WES) revealed that this patient had a germline *BRCA2* mutation and an *ASXL1* clonal hematopoiesis of indeterminate potential (CHIP) variant, while four other patients also carried variants in CHIP-associated genes (Table S2).

Two patients (6%) discontinued treatment before RP due to TRAEs, one due to grade 4 drug-induced liver injury and the other due to grade 3 hepatic function abnormality and insomnia. Dose reductions were necessary for four patients (11%). One patient required dose reductions of both fuzuloparib and abiraterone due to grade 3 hepatic function abnormalities. Two patients required a single-dose reduction of fuzuloparib for grade 2/3 anemia, and one patient required a dose reduction of abiraterone for grade 3 insomnia. Serious adverse events were reported in five patients (14%): two treatment-related (one drug-induced liver injury and one MDS) and three non-treatment-related (one diabetic nephropathy, one pneumonia, and one rib fracture).

Perioperative characteristics and complications are detailed in Table S3. Robotic-assisted RP was performed in 21 patients (66%), while laparoscopic RP was performed in 10 patients (31%). The most frequent perioperative complications were fever (56%, n = 18), urinary tract infection (6%, n = 2), and urine extravasation (6%, n = 2). There were no Clavien-Dindo grade $\geq$3 complications, and no patients required readmission or surgical reintervention within 90 days post surgery. Preoperative ultrasound examinations of patients' lower extremity deep veins revealed no thrombus formation.

Figure 1. Pathological response in the FAST-PC trial

(A) Pathological responses.

(B) Subgroup analyses of pathological responses in the intention-to-treat (ITT) population; data are presented as the pathological response rate (%) and 95% CI. pCR, pathological complete response; MRD, minimal residual disease.

(C) Representative pathological response of patients who achieved pCR or MRD before and after treatment (hematoxylin and eosin staining, along with confirmatory IHC for AE1/AE3 and p63). A black scale bar in the image represents 1 mm.

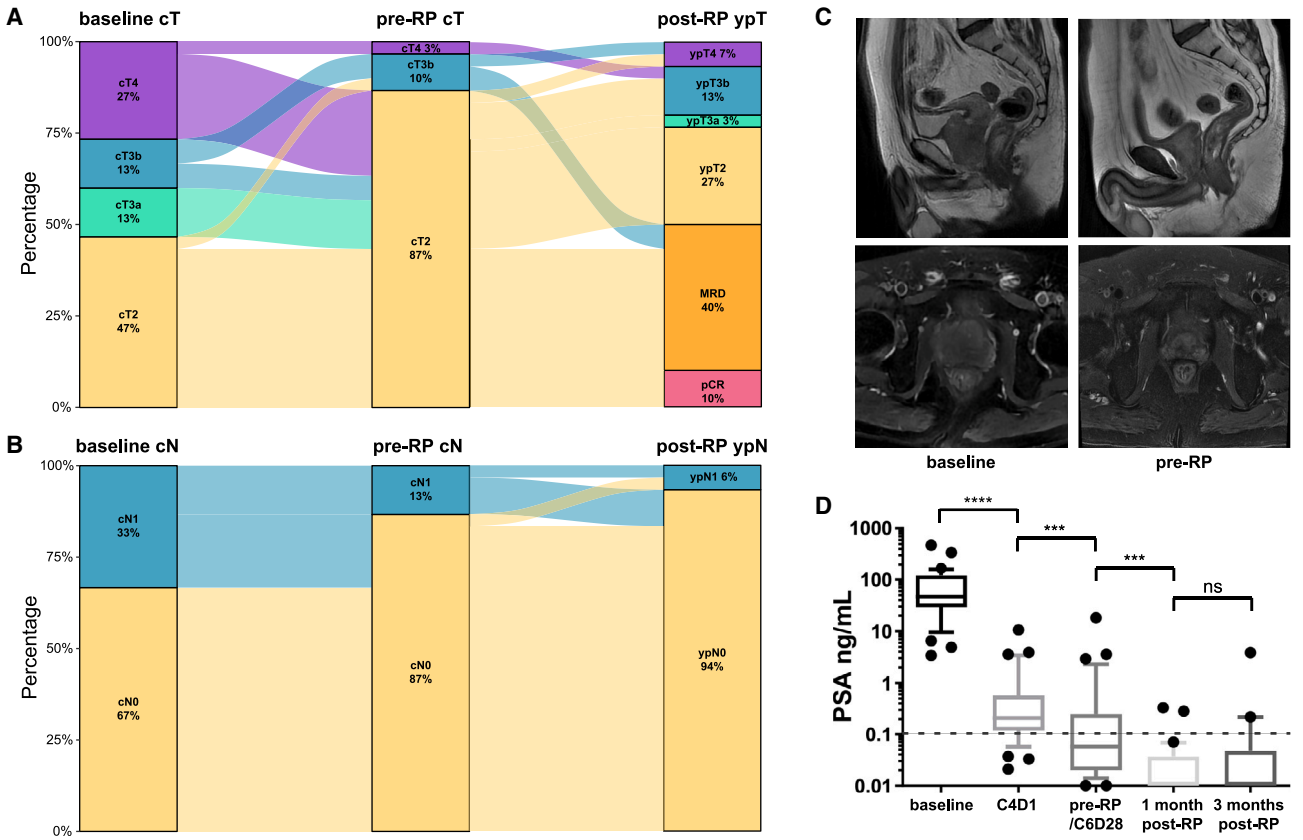

Figure 2. Radiologic and biochemical response in the FAST-PC trial

(A and B) The impact of neoadjuvant treatment on clinical TN stage (based on MRI) and correlation with pathological TN stage at final pathology (n = 30); three patients who did not receive RP at our hospital and two patients with missing post-treatment MRI data were excluded.

(C) Representative radiological response before and after neoadjuvant treatment using MRI (P34).

(D) Boxplots of the PSA level of the intention-to-treat population at baseline, following three cycles of neoadjuvant treatment, pre-RP, 1 month post RP, and 3 months post RP (n = 32–35); one PSA value 1 month post RP was missing due to loss to follow-up; two patients received RP following one cycle treatment due to adverse events, and their PSA values at the end of cycle 1 were measured at C4D1 and before RP; the PSA value was calculated as 0.01 ng/mL if it was equal to or lower than 0.01 ng/mL. The boxplot displays data distribution, where the bottom and top lines represent the minimum and maximum values (excluding outliers), the lower and upper edges of the box indicate the first and third quartiles, and the middle line within the box represents the median. Outliers, if present, are shown as individual points beyond the whiskers.

Statistical analysis was performed by the paired Wilcoxon test; ***$p < 0.001$, ****$p < 0.0001$; ns: non-significant, $p \geq 0.05$. RP, radical prostatectomy; MRI, magnetic resonance imaging; PSA, prostate-specific antigen; C4D1, day 1 of cycle 4; C6D28, day 28 of cycle 6.

Pre-treatment genomic characteristics and correlation with treatment response

Figure 5A illustrates the genomic landscape of the pre-treatment biopsy samples, matched with the baseline T stage and biochemical and pathological responses. Detected pathogenic variants within the FAST-PC cohort are detailed in Table S4. Among the genes of interest, *FOXA1* exhibited the highest frequency of genomic mutations (5/27, 19%), while *MYC* gain/amplification (14/27, 52%) and *RB1* shallow deletion (16/27, 59%) exhibited high frequencies of copy-number variants. Deleterious genomic alterations (pathogenic mutations and deep deletion) in the HRR pathway were observed in 10/27 patients (37%), including three germline *BRCA2* mutations and one *BRCA2* deep deletion. *TMPRSS2-ERG* fusion was detected in two patients (7%), and PTEN loss was identified in four patients (15%) (Figure S3).

WES data were utilized to calculate the homologous recombination deficiency (HRD) score, which assesses HRR deficiency. There was no significant difference in HRD scores between the HRR gene alteration group and the HRR gene wild-type group (p = 0.55). However, patients with *BRCA2* alterations had significantly higher HRD scores compared to those with wild-type *BRCA2* (p = 0.037). Despite this, the HRD score did not show a significant correlation with treatment response (Figure S4). We also calculated tumor mutational burden (TMB) and the fraction of genome altered (FGA). Patients with HRR gene alterations exhibited significantly higher TMB (p = 0.013) and a trend toward higher FGA (p = 0.26). Neither TMB nor FGA showed a significant correlation with treatment response (Figure S5). Notably, the sole patient (P11) who experienced disease progression during neoadjuvant treatment had the highest TMB

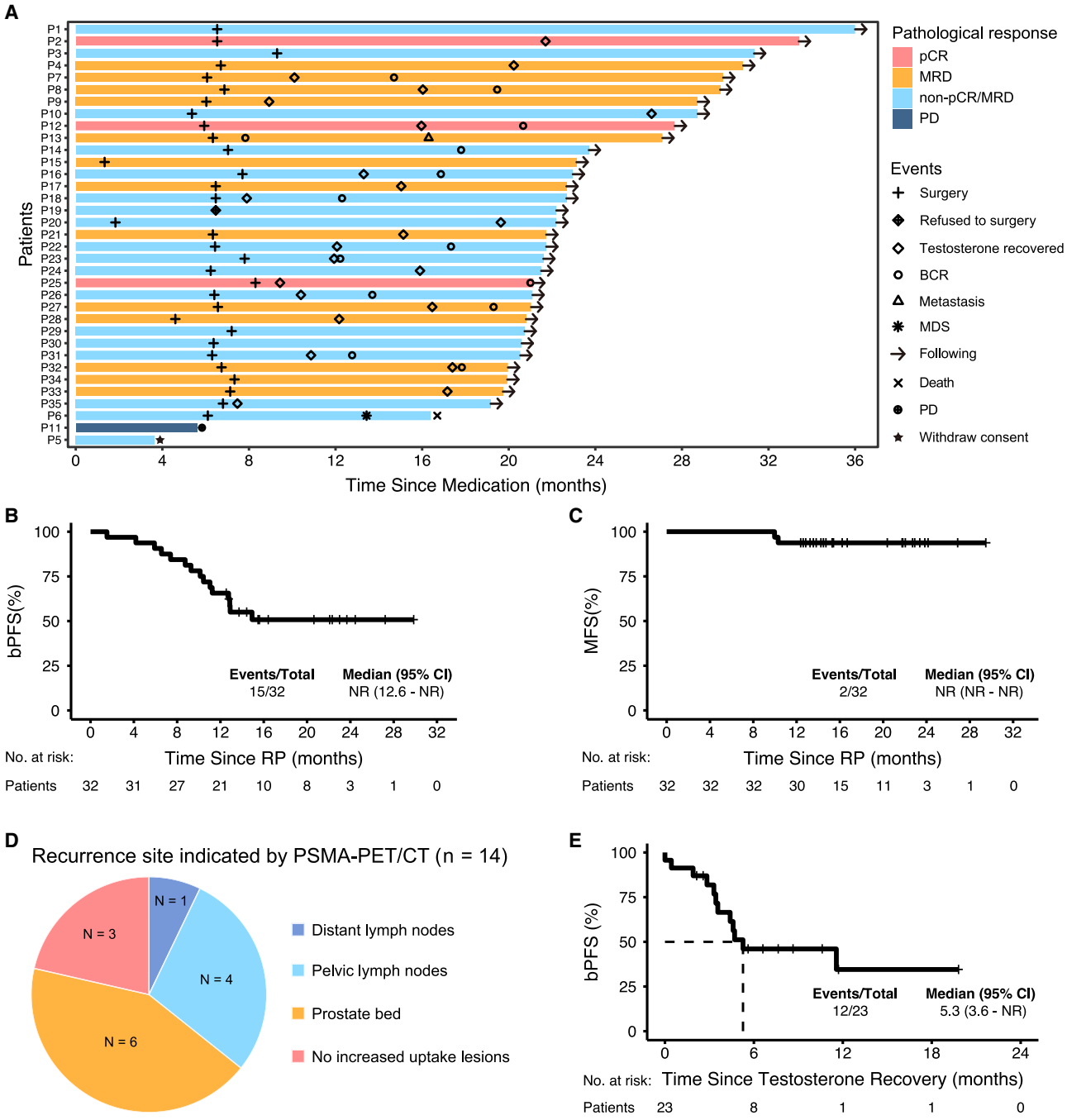

Figure 3. Follow-up of the FAST-PC trial

(A) Swimmer plot of 35 patients involved in the FAST-PC trial.

(B) Kaplan-Meier curves of bPFS for FAST-PC patients; one patient who withdrew consent and two patients who did not receive RP were excluded.

(C) Kaplan-Meier curves of MFS for FAST-PC patients; one patient who withdrew consent and two patients who did not receive RP were excluded.

(D) Recurrence site indicated by PSMA-PET/CT (n = 14).

(E) Kaplan-Meier curves of bPFS since testosterone recovery for patients who have undergone testosterone recovery. pCR, pathological complete response; MRD, minimal residual disease; PD, progressive disease; BCR, biochemical recurrence; MDS, myelodysplastic syndromes; bPFS, biochemical progression-free survival; RP, radical prostatectomy; MFS, metastasis-free survival; NR, not reached.

A

TRAE	All Grades	Grade 3	Grade 4	Grade 5
Any TRAE	33 (94%)	5 (14%)	1 (3%)	1 (3%)
Anemia	23 (66%)	2 (6%)		
Alanine aminotransferase increased	9 (26%)	1 (3%)		
Platelet count decreased	7 (20%)			
Hypokalemia	5 (14%)	1 (3%)		
Hepatic function abnormal	4 (11%)	2 (6%)		
Aspartate aminotransferase increased	4 (11%)	1 (3%)		
Blood bilirubin increased	4 (11%)			
Blood creatinine increased	3 (9%)			
White blood cell count decreased	2 (6%)			
Asthenia	2 (6%)			
Urinary tract infection	2 (6%)			
Myelodysplastic syndrome	1 (3%)			1 (3%)
Drug-induced liver injury	1 (3%)		1 (3%)	

B

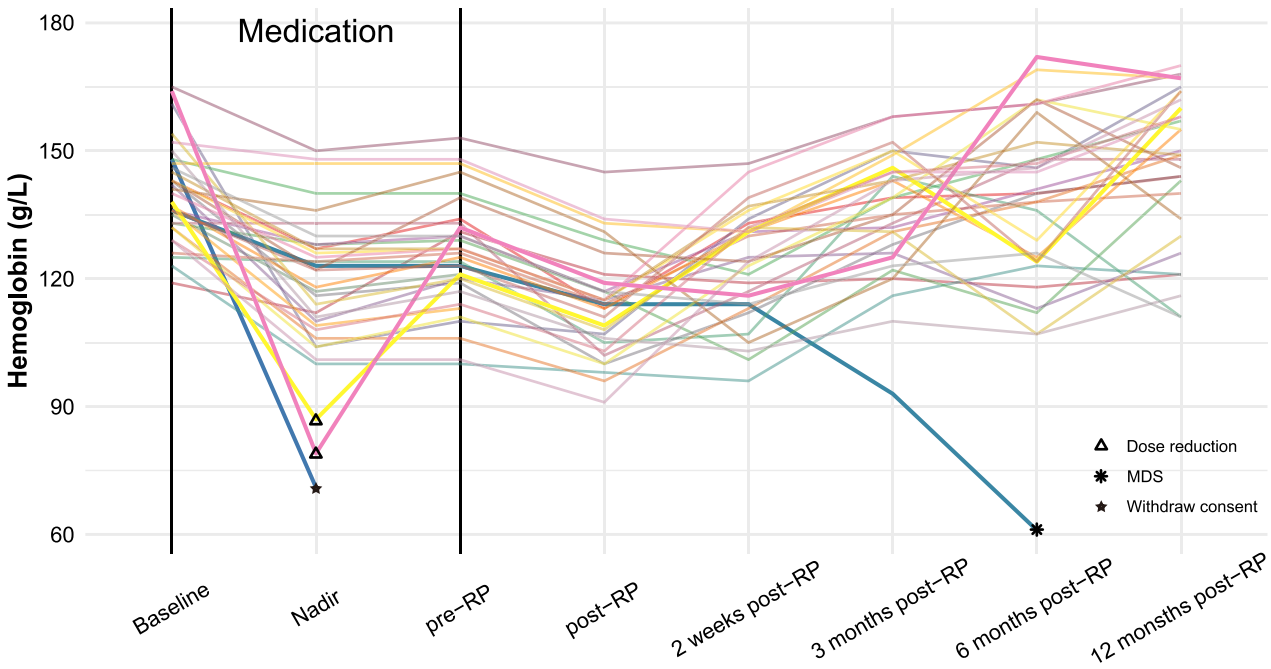

Figure 4. Treatment-related adverse events

(A) Treatment-related adverse events during medication.

(B) Hemoglobin levels; hemoglobin levels at baseline, nadir, pre-RP, post-RP, 2 weeks post RP, 3 months post RP, 6 months post-RP, and 12 months post RP; the thicker lines represent hemoglobin levels in patients with anemia that reached grade 2 or worse. TRAEs, treatment-related adverse events; RP, radical prostatectomy; MDS, myelodysplastic syndrome.

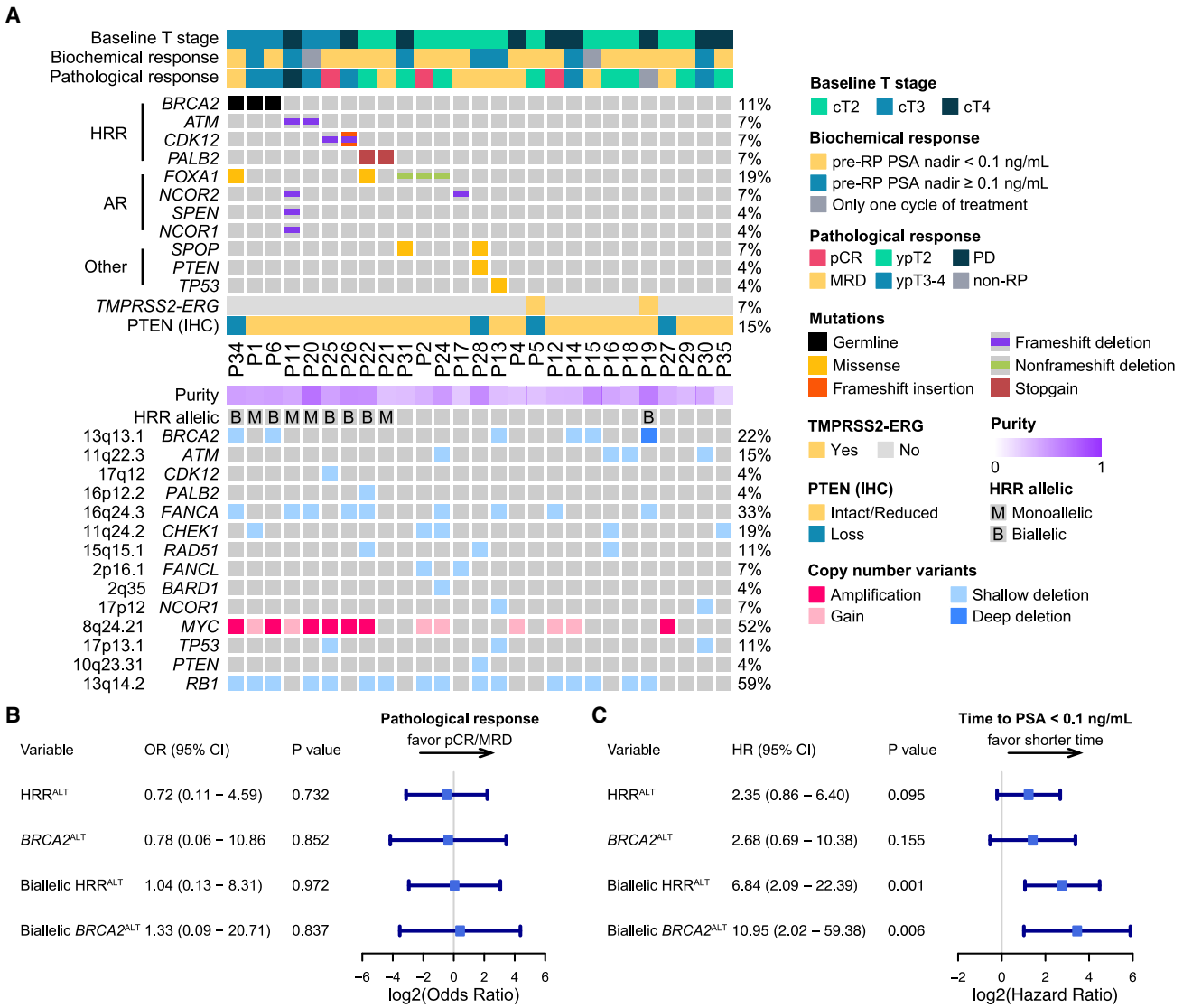

Figure 5. Pre-treatment molecular characteristics and correlation with treatment response

(A) Oncoplot showing mutations and copy-number variants as assessed by WES of baseline biopsy samples (n = 27).

(B) Correlation between HRR gene alterations and *BRCA2* alterations with pathological response, adjusted for baseline T stage.

(C) Correlation between HRR gene alterations and *BRCA2* alterations with time to achieve PSA level <0.1 ng/mL, adjusted for baseline PSA. HRR, homologous recombination repair; AR, androgen receptor; IHC, immunohistochemistry; PSA, prostate-specific antigen; pCR, pathological complete response; MRD, minimal residual disease; PD, progressive disease; RP, radical prostatectomy; ALT, alteration; OR, odds ratio; HR, hazard ratio.

(19.8 mutations/Mb) and was confirmed to have a dMMR status (Figure S6).

In our cohort, we assessed the allele status of HRR alterations (Table S5) and found that six out of 10 patients had biallelic HRR alterations, while three out of four patients had biallelic *BRCA2* alterations (Figure 5A). After adjusting for baseline T stage, neither HRR alterations nor *BRCA2* alterations, whether monoallelic or biallelic, were significantly associated with pathological response (Figure 5B). However, after adjusting for baseline PSA levels, patients with biallelic HRR alterations and *BRCA2* alterations demonstrated a shorter time to achieve PSA <0.1 ng/mL (p = 0.001 and p = 0.006, respectively, Figure 5C).

Genomic changes before and after treatment indicate potential sensitivity/tolerance mechanisms

Figure 6A presents the genomic characteristics of 19 patients with paired tissue samples collected before and after treatment. Most pathogenic mutations detected pre-treatment were not detected post-treatment, which was supported by the significantly reduced TMB after treatment (p < 0.001, Figure S7).

Interestingly, *MYC* gain/amplification, present in 42% of patients before treatment, was undetectable in paired post-treatment tissues (Figure 6A). RNA sequencing (RNA-seq) analysis of pre- and post-treatment tissues also confirmed a significant downregulation of *MYC* expression post treatment (p < 0.001).

CellPress
OPEN ACCESS

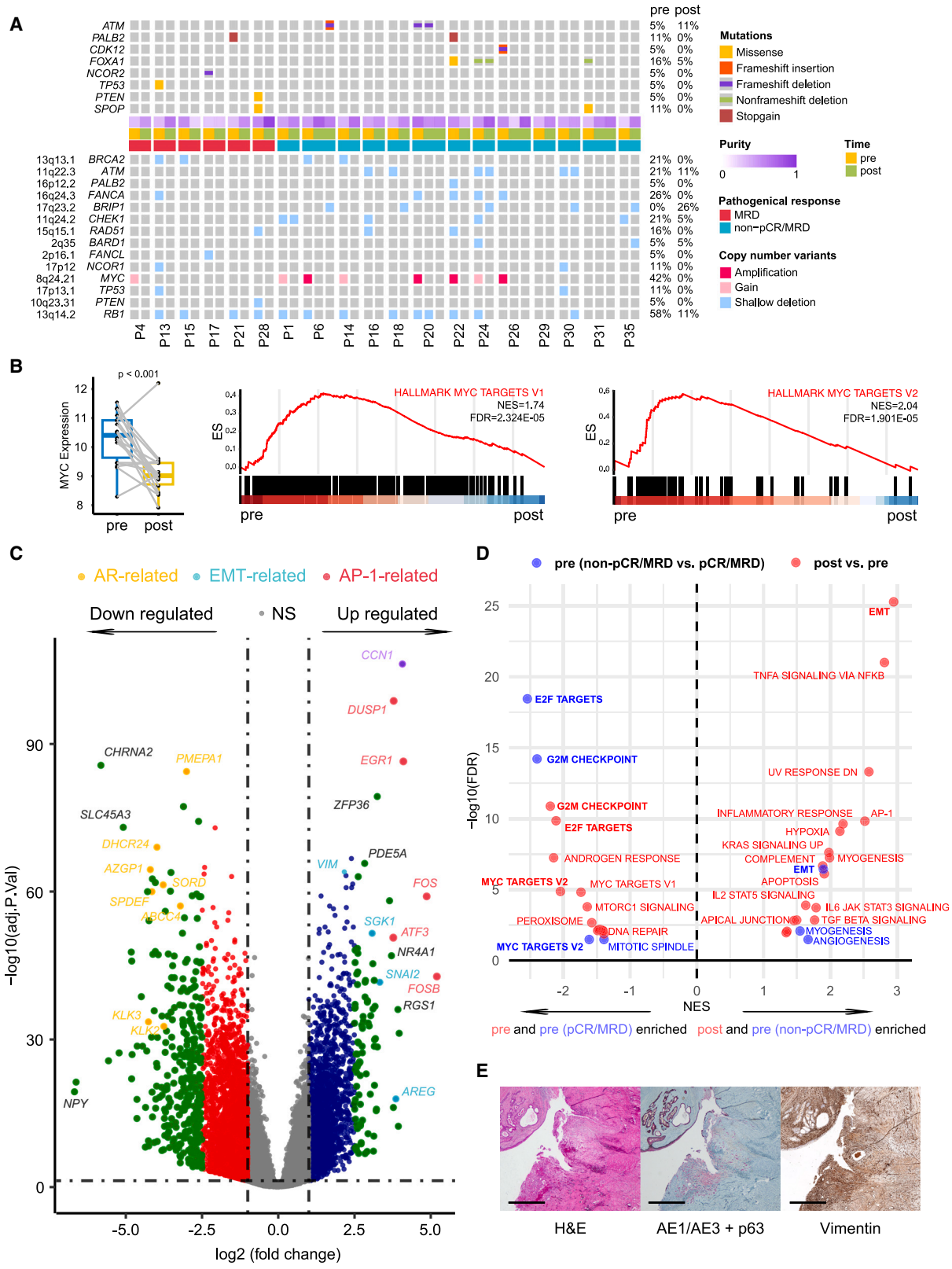

(legend on next page)

Gene set enrichment analysis (GSEA) further demonstrated that *MYC* target gene pathways were significantly suppressed following treatment (Figure 6B).

Subsequently, we conducted a comprehensive analysis of RNA-seq data from pre- and post-treatment specimens. Principal component analysis revealed a clear separation and significant transcriptomic distances between pre-treatment and post-treatment samples, as well as a homogeneous cluster among pCR/MRD and non-pCR/MRD samples before treatment (Figures S8A and S8B). Unsupervised hierarchical clustering corroborated these findings (Figure S8C).

The most differentially expressed genes are presented in Figure 6C. As anticipated, there was a marked downregulation of AR-related gene expression in post-treatment specimens, which corresponds with the downregulation observed in the hallmark androgen response pathway (false discovery rate = 5.76E−08, Figure S9A). Both ARG10 and the AR signature showed significant reductions post treatment and demonstrated a strong correlation (p = 1.26E−10, Figures S9B–S9D). The expression of *AR* did not significantly change before and after treatment (p = 0.865, Figure S9E), and no *AR* amplification was detected post treatment. The neuroendocrine score also showed no significant change pre- and post treatment (p = 0.442, Figure S9F). However, an increased expression of certain epithelial-to-mesenchymal transition (EMT) genes (*CCN1*, *VIM*, *SGK1*, *SNAI2*, and *AREG*) and activator protein 1 (AP-1)-related genes (*CCN1*, *DUSP1*, *EGR1*, *FOS*, *ATF3*, and *FOSB*) was noted in post-treatment specimens.

Next, we conducted GSEA comparing pCR/MRD samples to non-pCR/MRD samples before treatment, as well as pre- and post-treatment samples (Figure 6D). The pre-treatment comparison (blue) revealed that pCR/MRD specimens were enriched in E2F targets, G2M checkpoint, and MYC target pathways, suggesting increased tumor cell proliferation, while non-pCR/MRD specimens were enriched in the EMT pathway. These findings align with the overall patient characteristics before treatment and the residual tumor characteristics post treatment (red), indicating that factors influencing treatment sensitivity/tolerance may be present prior to treatment, with drug treatment reinforcing the selection of these features.

To confirm that the observed changes in post-treatment residual tumor cells reflect true EMT rather than an increased fraction of stromal cells, we performed vimentin immunohistochemical staining on post-treatment tissue samples. Our results demonstrate clear evidence of EMT within carcinoma cells, independent of the stromal component. Representative images, including H&E staining, AE1/AE3+p63 staining, and vimentin staining, are presented in Figure 6E to provide morphological evidence supporting our findings.

DISCUSSION

To our knowledge, the FAST-PC trial is the first prospective phase 2 trial to evaluate the efficacy, safety, and potential biomarkers of PARPi combined with ARSi in localized high-risk PCa. The trial met its primary endpoint, indicating promising antitumor activity with a pathological response rate of 46% and manageable toxicity associated with the neoadjuvant regimen of fuzuloparib, abiraterone, prednisone, and ADT in very high-risk patient population, for whom a multimodality treatment approach is strongly needed due to poor outcomes by conventional treatments.

A pooled analysis summarizing data from 201 patients with localized high-risk PCa who received neoadjuvant treatment with intensified ARSis reported an overall pathological response rate of 22.4% (95% CI: 16.8%–28.8%).[17] Comparing the baseline characteristics of our patients to those in these studies revealed a higher prevalence of high-risk factors in our cohort (Figure S10). Although cross-trial comparisons should be approached with caution, the combination of fuzuloparib, abiraterone, prednisone, and ADT demonstrated an increased pathological response rate in our cohort, despite the very high-risk features present. Since intensified ARSis are not the standard of care in the presurgical setting, we could not quantify the benefit of the combinations. Our study should be considered as signal-finding, and these benefits should be confirmed by randomized studies with long-term outcomes as endpoints. With a 2-year bPFS of 53% and a 2-year MFS of 94%, while only four patients received continuous adjuvant medical castration, the survival outcomes were favorable compared with the survival results from the STAMPEDE trial, in which the patients received continuous abiraterone and prednisolone with or without enzalutamide.[16] Patients in our study who achieved pCR/MRD showed numerically better testosterone-recovered bPFS (11.6 vs. 4.4 months), suggesting that sustained pathological response may be associated with better control of micrometastases. Given that 97% of our patients met the STAMPEDE high-risk criteria, abiraterone and ADT were considered the standard of care in addition to local treatment.[16] The favorable pathological response observed in our trial suggests that adding PARPi to the treatment regimen for these high-risk patients may enhance antitumor effects

Figure 6. Molecular changes before and after treatment indicate potential sensitivity/tolerance mechanisms

(A) Oncoplot showing mutations and copy-number variants of paired pre- and post-treatment samples (n = 19).

(B) Expression of *MYC* before and after treatment and enriched pathways of *MYC* target between pre- and post-treatment samples. The Benjamin-Hochberg method was used to calculate FDR adjusted p value for multiple comparisons; the boxplot displays data distribution, where the lower and upper edges of the box represent the first and third quartiles, and the middle line within the box represents the median. The whiskers extend to the minimum and maximum values within 1.5 times the interquartile range (IQR), while outliers, if present, are shown as individual points beyond the whiskers.

(C) Volcano plot showing differentially expressed genes between pre-treatment samples (n = 27) and post-treatment samples (n = 29). Color dots denote genes that passed the adjusted p value and fold change thresholds.

(D) GSEA comparing non-pCR/MRD samples to pCR/MRD samples before treatment (blue) and post-treatment samples to pre-treatment samples (red).

(E) Histopathological analysis of post-treatment tissues: H&E, AE1/AE3 + p63, and vimentin staining. A black scale bar in the image represents 1 mm. pCR, pathological complete response; MRD, minimal residual disease; NES, normalized enrichment score; FDR, false discovery rate; AR, androgen receptor; EMT, epithelial-to-mesenchymal transition; NS, not significant; H&E, hematoxylin and eosin.

and may be an attractive alternative to be tested in the future randomized trials.[18]

The neoadjuvant regimen comprising fuzuloparib, abiraterone, prednisone, and ADT demonstrated a relatively safe profile with manageable adverse events. The incidence of grade ≥3 TRAEs was relatively low and did not impede the surgical procedure. Hepatic toxicity and anemia were the most common grade ≥3 TRAEs. Specifically, grade ≥3 hepatic toxicity was observed in four out of 35 patients (11%), a rate comparable to that reported in patients receiving abiraterone alone for localized high-risk PCa.[19] Longitudinal monitoring of hemoglobin levels indicated a rapid recovery from anemia following a reduction in the fuzuloparib dose, and no blood transfusions were required. The risk of grade ≥3 anemia was numerically lower compared to the PROpel trial[10] in mCRPC (9% vs. 15%), despite the older age of our cohort, suggesting that patients without bone metastases and prior treatment may have an increased tolerance to PARPi.

Notably, a 76-year-old man with a germline *BRCA2* mutation and an *ASXL1* CHIP variant was diagnosed with MDS 7 months post RP, a known potential risk associated with PARPi treatment. The presence of CHIP in patients with solid tumors has been linked to an increased risk of subsequently developing therapy-related myeloid neoplasms like MDS and acute myeloid leukemia (AML).[20] Recent studies have shown an increase in CHIP following PARPi treatment in men with advanced PCa, which may underlie the association of PARPi treatment with the rare but serious side effects of MDS and AML.[21] Additional follow-up of men exposed to PARPis, especially those carrying CHIP, is needed to fully understand the long-term risks and complications.

Our translational analysis confirmed distinct genomic features of PCa among different races. Consistent with Li et al.,[22] Chinese patients exhibited a significantly lower probability of *PTEN* loss and *TMPRSS2-ERG* gene fusion, while showing a higher frequency of HRR pathway alterations, *FOXA1* mutations, *MYC* amplification, and *RB1* deletion.

We explored several candidate biomarkers for their correlations with biochemical and pathological response. Our studies demonstrated that biallelic HRR gene alterations and biallelic *BRCA2* alterations were significantly associated with a shorter time to achieve a PSA nadir of <0.1 ng/mL. This finding is consistent with previous studies indicating that inactivation of the second *BRCA* allele (biallelic) is associated with a better response to platinum/PARPi therapy.[23] Interestingly, three out of four *BRCA2* alterations were biallelic, while three out of six non-*BRCA2* HRR pathway alterations were biallelic. The differing allelic statuses may plausibly explain the varying benefits observed among patients with *BRCA* alterations and non-*BRCA* HRR pathway alterations.[24] Since patients with metastatic castrate-sensitive prostate cancer (mCSPC) may have multiple biopsy cores available for genomic sequencing, which are more likely to capture biallelic alterations compared to circulating tumor DNA,[25] ongoing phase 3 mCSPC trials (e.g., NCT04821622, NCT04497844, and NCT06120491) may include molecular stratification to test the hypothesis of better biochemical responses in patients with biallelic HRR alterations. It is noteworthy that the rate of pCR/MRD in patients with HRR pathway alterations or *BRCA2* alterations was comparable to those with wild-type tumors. This discordance may suggest that the combination therapy is more potent in eradicating micrometastases, while the primary tumor may develop drug-tolerant mechanisms to survive. In our study, we did not observe a significant correlation between baseline HRD scores in PCa tissue and treatment response to the combined therapy. Several factors could explain this observation. First, some patients with lower HRD scores still responded favorably to treatment, which may be due to their sensitivity to ARSi. Studies have suggested that ARSi might induce an HRD-like state, potentially enhancing sensitivity to PARPi in these patients. Second, certain patients with higher HRD scores had substantial residual tumor post treatment, indicating that additional mechanisms, such as EMT pathway upregulation, might be contributing to the persistence of tumor cells independently of the HRD score. Finally, the current HRD scoring systems were primarily developed in breast and ovarian cancers, where genomic landscapes differ from PCa. Limited research has validated HRD scoring in PCa, suggesting a need to develop PCa-specific HRD scoring models to better capture its unique genomic characteristics. Prostate-specific membrane antigen positron emission tomography/computed tomography (PSMA PET/CT) imaging at the time of recurrence also indicated that only one patient had distant metastases, while most had regional or local disease. Thus, it is intriguing to further investigate whether adjuvant radiotherapy, following neoadjuvant treatment and surgery, could improve the oncological outcomes.

Despite achieving a favorable biochemical response in the trial, with a median baseline PSA of 46.9 ng/mL, 54% of patients still presented with significant residual tumors (>5 mm). Paired analysis of pre- and post-treatment specimens provided insights into the dynamics of sensitive and tolerant clones. Notably, we observed a high rate of *MYC* clearance post treatment, consistent with findings in breast cancer studies.[26] Multiple studies have suggested that *MYC* enhances PARPi sensitivity by inducing DNA damage through alternative non-homologous end joining[27] or by impairing homologous recombination.[28] In line with *MYC* amplification, gene expression analysis revealed that pre-treatment samples from patients who achieved pCR/MRD were associated with the activation of E2F, G2M, and MYC pathways. These pathways were significantly downregulated in residual tumor samples post treatment, indicating either more proliferative tumors or tumors experiencing premature entry into the S phase and replication stress, both associated with PARPi[29,30] and ARSi[31] responsiveness.

Consistent with previous results from neoadjuvant ADT treatment results, AR pathway activity was significantly downregulated post treatment.[32,33] At the same time, there is no evidence of AR pathway resistance or neuroendocrine transformation following 6 months of ARSi combined with PARPi therapy.

Our analysis of pre- and post-treatment specimens indicated that tolerance to ARSi combined with PARPi therapy is characterized by an adaptive drug-tolerant persister intermediate EMT state in residual tumor cells. This phenotypic change mirrors those observed *in vitro* in human-derived PCa cells[34,35] and clinical trial patients.[29,31] Recent findings support that whereas EMT induction directly contributes to partial resistance, it more generally facilitates phenotypic plasticity over the long

term, enabling the emergence of additional mechanisms that increase drug resistance.[36] Importantly, EMT is not a one-way road but a highly dynamic and reversible process,[37] which also explains why patients remain sensitive to medical castration after recurrence in our trial. Our study is the first to clinically validate EMT as an intermediate state of resistance in trial specimens. Currently, numerous clinical trials are underway exploring therapies that inhibit EMT (e.g., NCT05546879, NCT05445791, NCT06203821, and NCT05550415), offering hope for further optimization of combined treatment strategies.

We observed an upregulation of AP-1-related genes post treatment. The members of AP-1 transcription factor family are key players in phenotypic plasticity as they coordinate global epigenetic and transcriptional changes, for instance during the acquisition of a partial EMT phenotype.[38] AP-1 is a druggable target for which multiple classes of small-molecule inhibitors have been developed.[39] Therefore, it is possible to consider therapeutically targeting AP-1 in the context of ARSi combined with PARPi therapy for the purpose of overcoming resistance.

In conclusion, the neoadjuvant regimen of fuzuloparib, abiraterone, prednisone, and ADT demonstrated favorable efficacy and manageable toxicity in patients with localized high-risk PCa. Our study identified that biallelic HRR pathway alterations and biallelic *BRCA2* alterations were associated with a shorter time to PSA nadir. There was a notable decrease in *MYC* gain/amplification and cell proliferation characteristics (E2F targets, G2M checkpoint, and MYC targets) following ARSi combined with PARPi therapy. Conversely, the activation of EMT and AP-1 was reinforced in drug-tolerant persister cells. Future trials are necessary to validate the clinical benefits of this combination and to explore interventions aimed at overcoming drug tolerance mechanisms following ARSi and PARPi combinations.

Limitations of the study

This study has several limitations. First, it employs a single-arm design with a relatively small sample size, necessitating cautious interpretation when comparing results with other neoadjuvant studies. Second, the molecular investigations represent post hoc analyses that require further validation in ongoing neoadjuvant PARPi trials (e.g., NCT05873192, NCT05498272, NCT04030559, and NCT04812366). Third, this study did not assess health-related quality of life, an important aspect for understanding the overall impact of the treatment. Finally, as our study primarily included patients from an Asian population, the findings may have limited generalizability to non-Asian populations.

RESOURCE AVAILABILITY

Lead contact

Further information and requests for resources should be directed to the lead contact, Yao Zhu (zhuyao@fudan.edu.cn).

Materials availability

This study did not generate new, unique reagents.

Data and code availability

The raw sequence data reported in this paper have been deposited in the Genome Sequence Archive (Genomics, Proteomics & Bioinformatics 2021) in National Genomic Data Center (Nucleic Acids Res 2022), China National Center for Bioinformation/Beijing Institute of Genomics, Chinese Academic Sciences (GSA-Human:HRA008404). Data access (http://ngdc.cncb.ac.cn/gsa-human) is subjected to the regulations by the Ministry of Science and Technology of the People's Republic of China.

This paper does not report original code. Any additional information required to reanalyze the data reported in this paper is available from the lead contact upon request.

ACKNOWLEDGMENTS

The authors are grateful to all patients and their families who participated in the study. The authors appreciate the support from Jiangsu Hengrui Pharmaceuticals. The authors also extend their gratitude to Professor Jun Luo from Johns Hopkins University School of Medicine and Professor Adam G. Sowalsky from National Cancer Institute for their advice on manuscript writing. The authors thank Bingni Zhou for evaluating the imaging data and Xu Cai for assessing the pathological data. Additionally, the authors appreciate the support provided by the Medical Science Data Center in Shanghai Medical College of Fudan University. This work was supported by the National Natural Science Foundation of China (82172621, 81972375, 82473381, 82203106, and 823B2066), the Shanghai Medical Innovation Research Special Project (21Y11904300), the General Program of Beijing Xisike Clinical Oncology Research Foundation (Y-MSDZD2021-0230), the Chinese Anti-Cancer Association-Hengrui PARP Inhibitor Tumor Research Fund (Phase I), the Program of Shanghai Academic Research Leader (23XD1420600), the Program for Professor of Special Appointment (Easter Scholar) (TP2022051), Beijing Weikang Prostate Cancer Research Special Fund (WK2024-003), and the Shanghai Shenkang Research Physician Innovation and Transformation Ability Training Project (SHDC2022CRD035).

AUTHOR CONTRIBUTIONS

Conceptualization, D.Y. and Y.Z.; methodology, T.Z., B.W., Y.W., H.G., S.H., and Y.Z.; formal analysis, T.Z. and S.H.; investigation, B.F., X.L., X.B., and S.J.F.; writing – original draft, T.Z., B.W., Y.W., J.Wu, and Y.Z.; writing – review and editing, T.Z., J.W., and Y.Z.; resources, J.Wang, D.Y., and Y.Z.; visualization, T.Z.; supervision, J.Wang, D.Y., and Y.Z.; funding acquisition, B.W. and Y.Z. D.Y. and Y.Z. had unrestricted access to all data. All authors approved the final manuscript and take full responsibility for its content, including data accuracy and adherence to the registered protocol and statistical analysis.

DECLARATION OF INTERESTS

The authors declare no competing interests.

STAR★METHODS

Detailed methods are provided in the online version of this paper and include the following:

- KEY RESOURCES TABLE
- EXPERIMENTAL MODEL AND STUDY PARTICIPANT DETAILS
  - Study design and participants
  - Procedures
  - Outcomes
- METHOD DETAILS
  - Exploratory analyses
  - DNA and RNA extraction
  - Whole-exome sequencing
  - Variant calling
  - Pathogenicity for mutations
  - CHIP definition
  - Copy number evaluation
  - HRR allelic
  - HRD score, TMB and FGA
  - RNA-seq

- Differentially expressed genes and pathway enrichment analysis
- ARG10, AR signature, and NE score
- PCA and unsupervised clustering
- PTEN immunohistochemistry

- QUANTIFICATION AND STATISTICAL ANALYSIS
- ADDITIONAL RESOURCES

SUPPLEMENTAL INFORMATION

Supplemental information can be found online at https://doi.org/10.1016/j.xcrm.2025.102018.

Received: August 6, 2024
Revised: December 19, 2024
Accepted: February 17, 2025
Published: March 7, 2025

REFERENCES

1. Tilki, D., Chen, M.H., Wu, J., Huland, H., Graefen, M., Braccioforte, M., Moran, B.J., and D'Amico, A.V. (2019). Surgery vs Radiotherapy in the Management of Biopsy Gleason Score 9-10 Prostate Cancer and the Risk of Mortality. JAMA Oncol. *5*, 213–220. https://doi.org/10.1001/jamaoncol.2018.4836.
2. Ravi, P. (2023). Refining Risk Stratification in Patients Undergoing Radiotherapy and Long-Term ADT for High-Risk/locally Advanced Prostate Cancer: An Individual Patient Data Analysis of RCTs from the ICECaP Consortium. ESMO *43*, 2023.
3. National Comprehensive Cancer Network (2023). Clinical Practice Guidelines in Oncology Prostate Cancer Version 4.2023.. https://www.nccn.org/professionals/physician_gls/pdf/prostate.
4. Dai, B., Wang, H., Shi, B., Xing, J., Zhu, S., He, Z., Zou, Q., Wei, Q., Bi, J., Bian, J., et al. (2024). CACA guidelines for holistic integrative management of prostate cancer. Holist. Integr. Oncol. *3*, 47. https://doi.org/10.1007/s44178-024-00118-4.
5. Shelley, M.D., Kumar, S., Wilt, T., Staffurth, J., Coles, B., and Mason, M.D. (2009). A systematic review and meta-analysis of randomised trials of neoadjuvant hormone therapy for localised and locally advanced prostate carcinoma. Cancer Treat Rev. *35*, 9–17. https://doi.org/10.1016/j.ctrv.2008.08.002.
6. Fraser, M., Sabelnykova, V.Y., Yamaguchi, T.N., Heisler, L.E., Livingstone, J., Huang, V., Shiah, Y.J., Yousif, F., Lin, X., Masella, A.P., et al. (2017). Genomic hallmarks of localized, non-indolent prostate cancer. Nature *541*, 359–364. https://doi.org/10.1038/nature20788.
7. Cancer Genome Atlas Research Network (2015). The Molecular Taxonomy of Primary Prostate Cancer. Cellule *163*, 1011–1025. https://doi.org/10.1016/j.cell.2015.10.025.
8. Castro, E., Goh, C., Olmos, D., Saunders, E., Leongamornlert, D., Tymrakiewicz, M., Mahmud, N., Dadaev, T., Govindasami, K., Guy, M., et al. (2013). Germline BRCA mutations are associated with higher risk of nodal involvement, distant metastasis, and poor survival outcomes in prostate cancer. J. Clin. Oncol. *31*, 1748–1757. https://doi.org/10.1200/JCO.2012.43.1882.
9. Asim, M., Tarish, F., Zecchini, H.I., Sanjiv, K., Gelali, E., Massie, C.E., Baridi, A., Warren, A.Y., Zhao, W., Ogris, C., et al. (2017). Synthetic lethality between androgen receptor signalling and the PARP pathway in prostate cancer. Nat. Commun. *8*, 374. https://doi.org/10.1038/s41467-017-00393-y.
10. Saad, F., Clarke, N.W., Oya, M., Shore, N., Procopio, G., Guedes, J.D., Arslan, C., Mehra, N., Parnis, F., Brown, E., et al. (2023). Olaparib plus abiraterone versus placebo plus abiraterone in metastatic castration-resistant prostate cancer (PROpel): final prespecified overall survival results of a randomised, double-blind, phase 3 trial. Lancet Oncol. *24*, 1094–1108. https://doi.org/10.1016/S1470-2045(23)00382-0.
11. Agarwal, N., Azad, A.A., Carles, J., Fay, A.P., Matsubara, N., Heinrich, D., Szczylik, C., De Giorgi, U., Young Joung, J., Fong, P.C.C., et al. (2023). Talazoparib plus enzalutamide in men with first-line metastatic castration-resistant prostate cancer (TALAPRO-2): a randomised, placebo-controlled, phase 3 trial. Lancet *402*, 291–303. https://doi.org/10.1016/S0140-6736(23)01055-3.
12. Chi, K.N., Rathkopf, D., Smith, M.R., Efstathiou, E., Attard, G., Olmos, D., Lee, J.Y., Small, E.J., Pereira de Santana Gomes, A.J., Roubaud, G., et al. (2023). Niraparib and Abiraterone Acetate for Metastatic Castration-Resistant Prostate Cancer. J. Clin. Oncol. *41*, 3339–3351. https://doi.org/10.1200/JCO.22.01649.
13. Li, L., Karanika, S., Yang, G., Wang, J., Park, S., Broom, B.M., Manyam, G.C., Wu, W., Luo, Y., Basourakos, S., et al. (2017). Androgen receptor inhibitor-induced "BRCAness" and PARP inhibition are synthetically lethal for castration-resistant prostate cancer. Sci. Signal. *10*, eaam7479. https://doi.org/10.1126/scisignal.aam7479.
14. Wang, L., Yang, C., Xie, C., Jiang, J., Gao, M., Fu, L., Li, Y., Bao, X., Fu, H., and Lou, L. (2019). Pharmacologic characterization of fluzoparib, a novel poly(ADP-ribose) polymerase inhibitor undergoing clinical trials. Cancer Sci. *110*, 1064–1075. https://doi.org/10.1111/cas.13947.
15. Li, N., Zhang, Y., Wang, J., Zhu, J., Wang, L., Wu, X., Yao, D., Wu, Q., Liu, J., Tang, J., et al. (2022). Fuzuloparib Maintenance Therapy in Patients With Platinum-Sensitive, Recurrent Ovarian Carcinoma (FZOCUS-2): A Multicenter, Randomized, Double-Blind, Placebo-Controlled, Phase III Trial. J. Clin. Oncol. *40*, 2436–2446. https://doi.org/10.1200/JCO.21.01511.
16. Attard, G., Murphy, L., Clarke, N.W., Cross, W., Jones, R.J., Parker, C.C., Gillessen, S., Cook, A., Brawley, C., Amos, C.L., et al. (2022). Abiraterone acetate and prednisolone with or without enzalutamide for high-risk non-metastatic prostate cancer: a meta-analysis of primary results from two randomised controlled phase 3 trials of the STAMPEDE platform protocol. Lancet *399*, 447–460. https://doi.org/10.1016/S0140-6736(21)02437-5.
17. Berchuck, J.E., Zhang, Z., Silver, R., Kwak, L., Xie, W., Lee, G.S.M., Freedman, M.L., Kibel, A.S., Van Allen, E.M., McKay, R.R., and Taplin, M.E. (2021). Impact of Pathogenic Germline DNA Damage Repair alterations on Response to Intense Neoadjuvant Androgen Deprivation Therapy in High-risk Localized Prostate Cancer. Eur. Urol. *80*, 295–303. https://doi.org/10.1016/j.eururo.2021.03.031.
18. Xie, W., Regan, M.M., Buyse, M., Halabi, S., Kantoff, P.W., Sartor, O., Soule, H., Clarke, N.W., Collette, L., Dignam, J.J., et al. (2017). Metastasis-Free Survival Is a Strong Surrogate of Overall Survival in Localized Prostate Cancer. J. Clin. Oncol. *35*, 3097–3104. https://doi.org/10.1200/jco.2017.73.9987.
19. Taplin, M.E., Montgomery, B., Logothetis, C.J., Bubley, G.J., Richie, J.P., Dalkin, B.L., Sanda, M.G., Davis, J.W., Loda, M., True, L.D., et al. (2014). Intense androgen-deprivation therapy with abiraterone acetate plus leuprolide acetate in patients with localized high-risk prostate cancer: results of a randomized phase II neoadjuvant study. J. Clin. Oncol. *32*, 3705–3715. https://doi.org/10.1200/JCO.2013.53.4578.
20. Gillis, N.K., Ball, M., Zhang, Q., Ma, Z., Zhao, Y., Yoder, S.J., Balasis, M.E., Mesa, T.E., Sallman, D.A., Lancet, J.E., et al. (2017). Clonal haemopoiesis and therapy-related myeloid malignancies in elderly patients: a proof-of-concept, case-control study. Lancet Oncol. *18*, 112–121. https://doi.org/10.1016/S1470-2045(16)30627-1.
21. Marshall, C.H., Gondek, L.P., Daniels, V., Lu, C., Pasca, S., Xie, J., Markowski, M.C., Paller, C.J., Sena, L.A., Denmeade, S.R., et al. (2024). Association of PARP inhibitor treatment on the prevalence and progression of clonal hematopoiesis in patients with advanced prostate cancer. Prostate *84*, 954–958. https://doi.org/10.1002/pros.24712.
22. Li, J., Xu, C., Lee, H.J., Ren, S., Zi, X., Zhang, Z., Wang, H., Yu, Y., Yang, C., Gao, X., et al. (2020). A genomic and epigenomic atlas of prostate cancer in Asian populations. Nature *580*, 93–99. https://doi.org/10.1038/s41586-020-2135-x.

23. Waddell, N., Pajic, M., Patch, A.M., Chang, D.K., Kassahn, K.S., Bailey, P., Johns, A.L., Miller, D., Nones, K., Quek, K., et al. (2015). Whole genomes redefine the mutational landscape of pancreatic cancer. Nature *518*, 495–501. https://doi.org/10.1038/nature14169.

24. Fallah, J., Xu, J., Weinstock, C., Gao, X., Heiss, B.L., Maguire, W.F., Chang, E., Agrawal, S., Tang, S., Amiri-Kordestani, L., et al. (2024). Efficacy of Poly(ADP-ribose) Polymerase Inhibitors by Individual Genes in Homologous Recombination Repair Gene-Mutated Metastatic Castration-Resistant Prostate Cancer: A US Food and Drug Administration Pooled Analysis. J. Clin. Oncol. *42*, 1687–1698. https://doi.org/10.1200/JCO.23.02105.

25. Warner, E.W., Van der Eecken, K., Murtha, A.J., Kwan, E.M., Herberts, C., Sipola, J., Ng, S.W.S., Chen, X.E., Fonseca, N.M., Ritch, E., et al. (2024). Multiregion sampling of de novo metastatic prostate cancer reveals complex polyclonality and augments clinical genotyping. Nat. Can. (Ott.) *5*, 114–130. https://doi.org/10.1038/s43018-023-00692-y.

26. Lin, C.J., Jin, X., Ma, D., Chen, C., Ou-Yang, Y., Pei, Y.C., Zhou, C.Z., Qu, F.L., Wang, Y.J., Liu, C.L., et al. (2024). Genetic interactions reveal distinct biological and therapeutic implications in breast cancer. Cancer Cell *42*, 701–719.e12. https://doi.org/10.1016/j.ccell.2024.03.006.

27. Caracciolo, D., Scionti, F., Juli, G., Altomare, E., Golino, G., Todoerti, K., Grillone, K., Riillo, C., Arbitrio, M., Iannone, M., et al. (2021). Exploiting MYC-induced PARPness to target genomic instability in multiple myeloma. Haematologica *106*, 185–195. https://doi.org/10.3324/haematol.2019.240713.

28. Ning, J.F., Stanciu, M., Humphrey, M.R., Gorham, J., Wakimoto, H., Nishihara, R., Lees, J., Zou, L., Martuza, R.L., Wakimoto, H., and Rabkin, S.D. (2019). Myc targeted CDK18 promotes ATR and homologous recombination to mediate PARP inhibitor resistance in glioblastoma. Nat. Commun. *10*, 2910. https://doi.org/10.1038/s41467-019-10993-5.

29. Liu, X., Ge, Z., Yang, F., Contreras, A., Lee, S., White, J.B., Lu, Y., Labrie, M., Arun, B.K., Moulder, S.L., et al. (2022). Identification of biomarkers of response to preoperative talazoparib monotherapy in treatment naive gBRCA+ breast cancers. NPJ Breast Cancer *8*, 64. https://doi.org/10.1038/s41523-022-00427-9.

30. Fang, Y., McGrail, D.J., Sun, C., Labrie, M., Chen, X., Zhang, D., Ju, Z., Vellano, C.P., Lu, Y., Li, Y., et al. (2019). Sequential Therapy with PARP and WEE1 Inhibitors Minimizes Toxicity while Maintaining Efficacy. Cancer Cell *35*, 851–867.e7. https://doi.org/10.1016/j.ccell.2019.05.001.

31. Lee, L.S., Sim, A.Y.L., Ong, C.W., Yang, X., Ng, C.C.Y., Liu, W., Rajasegaran, V., Lim, A.M.S., Aslim, E.J., Ngo, N.T., et al. (2022). NEAR trial: A single-arm phase II trial of neoadjuvant apalutamide monotherapy and radical prostatectomy in intermediate- and high-risk prostate cancer. Prostate Cancer Prostatic Dis. *25*, 741–748. https://doi.org/10.1038/s41391-022-00496-8.

32. Beltran, H., Wyatt, A.W., Chedgy, E.C., Donoghue, A., Annala, M., Warner, E.W., Beja, K., Sigouros, M., Mo, F., Fazli, L., et al. (2017). Impact of Therapy on Genomics and Transcriptomics in High-Risk Prostate Cancer Treated with Neoadjuvant Docetaxel and Androgen Deprivation Therapy. Clin. Cancer Res. *23*, 6802–6811. https://doi.org/10.1158/1078-0432.CCR-17-1034.

33. Sowalsky, A.G., Ye, H., Bhasin, M., Van Allen, E.M., Loda, M., Lis, R.T., Montaser-Kouhsari, L., Calagua, C., Ma, F., Russo, J.W., et al. (2018). Neoadjuvant-Intensive Androgen Deprivation Therapy Selects for Prostate Tumor Foci with Diverse Subclonal Oncogenic Alterations. Cancer Res. *78*, 4716–4730. https://doi.org/10.1158/0008-5472.CAN-18-0610.

34. Huo, C., Kao, Y.H., and Chuu, C.P. (2015). Androgen receptor inhibits epithelial-mesenchymal transition, migration, and invasion of PC-3 prostate cancer cells. Cancer Lett. *369*, 103–111. https://doi.org/10.1016/j.canlet.2015.08.001.

35. Zhu, M.L., and Kyprianou, N. (2010). Role of androgens and the androgen receptor in epithelial-mesenchymal transition and invasion of prostate cancer cells. FASEB J. *24*, 769–777. https://doi.org/10.1096/fj.09-136994.

36. Franca, G.S., Baron, M., King, B.R., Bossowski, J.P., Bjornberg, A., Pour, M., Rao, A., Patel, A.S., Misirlioglu, S., Barkley, D., et al. (2024). Cellular adaptation to cancer therapy along a resistance continuum. Nature *631*, 876–883. https://doi.org/10.1038/s41586-024-07690-9.

37. Chaffer, C.L., San Juan, B.P., Lim, E., and Weinberg, R.A. (2016). EMT, cell plasticity and metastasis. Cancer Metastasis Rev. *35*, 645–654. https://doi.org/10.1007/s10555-016-9648-7.

38. Ervin, E.H., French, R., Chang, C.H., and Pauklin, S. (2022). Inside the stemness engine: Mechanistic links between deregulated transcription factors and stemness in cancer. Semin. Cancer Biol. *87*, 48–83. https://doi.org/10.1016/j.semcancer.2022.11.001.

39. Song, D., Lian, Y., and Zhang, L. (2023). The potential of activator protein 1 (AP-1) in cancer targeted therapy. Front. Immunol. *14*, 1224892. https://doi.org/10.3389/fimmu.2023.1224892.

40. Common Terminology Criteria for Adverse Events (CTCAE) Version 5.0. (2017). In U.S. DEPARTMENT OF HEALTH AND HUMAN SERVICES, ed.

41. Clavien, P.A., Barkun, J., de Oliveira, M.L., Vauthey, J.N., Dindo, D., Schulick, R.D., de Santibañes, E., Pekolj, J., Slankamenac, K., Bassi, C., et al. (2009). The Clavien-Dindo classification of surgical complications: five-year experience. Ann. Surg. *250*, 187–196. https://doi.org/10.1097/SLA.0b013e3181b13ca2.

42. Espiritu, S.M.G., Liu, L.Y., Rubanova, Y., Bhandari, V., Holgersen, E.M., Szyca, L.M., Fox, N.S., Chua, M.L.K., Yamaguchi, T.N., Heisler, L.E., et al. (2018). The Evolutionary Landscape of Localized Prostate Cancers Drives Clinical Aggression. Cell *173*, 1003–1013.e15. https://doi.org/10.1016/j.cell.2018.03.029.

43. Cooper, C.S., Eeles, R., Wedge, D.C., Van Loo, P., Gundem, G., Alexandrov, L.B., Kremeyer, B., Butler, A., Lynch, A.G., Camacho, N., et al. (2015). Analysis of the genetic phylogeny of multifocal prostate cancer identifies multiple independent clonal expansions in neoplastic and morphologically normal prostate tissue. Nat. Genet. *47*, 367–372. https://doi.org/10.1038/ng.3221.

44. Pan, J., Wu, J., Wang, B., Zhu, B., Liu, X., Gan, H., Wei, Y., Jin, S., Hu, X., Wang, Q., et al. (2024). Interlesional response heterogeneity is associated with the prognosis of abiraterone treatment in metastatic castration-resistant prostate cancer. Medizinrecht *5*, 1475–1484.e3. https://doi.org/10.1016/j.medj.2024.07.020.

45. Shen, R., and Seshan, V.E. (2016). FACETS: allele-specific copy number and clonal heterogeneity analysis tool for high-throughput DNA sequencing. Nucleic Acids Res. *44*, e131. https://doi.org/10.1093/nar/gkw520.

46. Fan, X., Luo, G., and Huang, Y.S. (2021). Accucopy: accurate and fast inference of allele-specific copy number alterations from low-coverage low-purity tumor sequencing data. BMC Bioinf. *22*, 23. https://doi.org/10.1186/s12859-020-03924-5.

47. Landrum, M.J., Lee, J.M., Riley, G.R., Jang, W., Rubinstein, W.S., Church, D.M., and Maglott, D.R. (2014). ClinVar: public archive of relationships among sequence variation and human phenotype. Nucleic Acids Res. *42*, D980–D985. https://doi.org/10.1093/nar/gkt1113.

48. Li, Q., and Wang, K. (2017). InterVar: Clinical Interpretation of Genetic Variants by the 2015 ACMG-AMP Guidelines. Am. J. Hum. Genet. *100*, 267–280. https://doi.org/10.1016/j.ajhg.2017.01.004.

49. Chakravarty, D., Gao, J., Phillips, S.M., Kundra, R., Zhang, H., Wang, J., Rudolph, J.E., Yaeger, R., Soumerai, T., Nissan, M.H., et al. (2017). OncoKB: A Precision Oncology Knowledge Base. JCO Precis. Oncol. *1*, 1–16. https://doi.org/10.1200/PO.17.00011.

50. Quigley, D.A., Dang, H.X., Zhao, S.G., Lloyd, P., Aggarwal, R., Alumkal, J.J., Foye, A., Kothari, V., Perry, M.D., Bailey, A.M., et al. (2018). Genomic Hallmarks and Structural Variation in Metastatic Prostate Cancer. Cell *174*, 758–769.e9. https://doi.org/10.1016/j.cell.2018.06.039.

51. Abida, W., Armenia, J., Gopalan, A., Brennan, R., Walsh, M., Barron, D., Danila, D., Rathkopf, D., Morris, M., Slovin, S., et al. (2017). Prospective Genomic Profiling of Prostate Cancer Across Disease States Reveals

Germline and Somatic Alterations That May Affect Clinical Decision Making. JCO Precis. Oncol. *1*, 1–16. https://doi.org/10.1200/PO.17.00029.

52. Menssouri, N., Poiraudeau, L., Helissey, C., Bigot, L., Sabio, J., Ibrahim, T., Pobel, C., Nicotra, C., Ngo-Camus, M., Lacroix, L., et al. (2023). Genomic profiling of metastatic castration-resistant prostate cancer samples resistant to androgen-receptor pathway inhibitors. Clin. Cancer Res. *29*, 4504–4517. https://doi.org/10.1158/1078-0432.CCR-22-3736.
53. Tewari, A.K., Cheung, A.T.M., Crowdis, J., Conway, J.R., Camp, S.Y., Wankowicz, S.A., Livitz, D.G., Park, J., Lis, R.T., Bosma-Moody, A., et al. (2021). Molecular features of exceptional response to neoadjuvant anti-androgen therapy in high-risk localized prostate cancer. Cell Rep. *36*, 109665. https://doi.org/10.1016/j.celrep.2021.109665.
54. Warner, E., Herberts, C., Fu, S., Yip, S., Wong, A., Wang, G., Ritch, E., Murtha, A.J., Vandekerkhove, G., Fonseca, N.M., et al. (2021). BRCA2, ATM, and CDK12 Defects Differentially Shape Prostate Tumor Driver Genomics and Clinical Aggression. Clin. Cancer Res. *27*, 1650–1662. https://doi.org/10.1158/1078-0432.CCR-20-3708.
55. Sztupinszki, Z., Diossy, M., Krzystanek, M., Reiniger, L., Csabai, I., Favero, F., Birkbak, N.J., Eklund, A.C., Syed, A., and Szallasi, Z. (2018). Migrating the SNP array-based homologous recombination deficiency measures to next generation sequencing data of breast cancer. NPJ Breast Cancer *4*, 16. https://doi.org/10.1038/s41523-018-0066-6.
56. Liberzon, A., Birger, C., Thorvaldsdóttir, H., Ghandi, M., Mesirov, J.P., and Tamayo, P. (2015). The Molecular Signatures Database (MSigDB) hallmark gene set collection. Cell Syst. *1*, 417–425. https://doi.org/10.1016/j.cels.2015.12.004.
57. Schaefer, C.F., Anthony, K., Krupa, S., Buchoff, J., Day, M., Hannay, T., and Buetow, K.H. (2009). PID: the Pathway Interaction Database. Nucleic Acids Res. *37*, D674–D679. https://doi.org/10.1093/nar/gkn653.
58. Westbrook, T.C., Guan, X., Rodansky, E., Flores, D., Liu, C.J., Udager, A.M., Patel, R.A., Haffner, M.C., Hu, Y.M., Sun, D., et al. (2022). Transcriptional profiling of matched patient biopsies clarifies molecular determinants of enzalutamide-induced lineage plasticity. Nat. Commun. *13*, 5345. https://doi.org/10.1038/s41467-022-32701-6.
59. Nyquist, M.D., Corella, A., Coleman, I., De Sarkar, N., Kaipainen, A., Ha, G., Gulati, R., Ang, L., Chatterjee, P., Lucas, J., et al. (2020). Combined TP53 and RB1 Loss Promotes Prostate Cancer Resistance to a Spectrum of Therapeutics and Confers Vulnerability to Replication Stress. Cell Rep. *31*, 107669. https://doi.org/10.1016/j.celrep.2020.107669.
60. Hieronymus, H., Lamb, J., Ross, K.N., Peng, X.P., Clement, C., Rodina, A., Nieto, M., Du, J., Stegmaier, K., Raj, S.M., et al. (2006). Gene expression signature-based chemical genomic prediction identifies a novel class of HSP90 pathway modulators. Cancer Cell *10*, 321–330. https://doi.org/10.1016/j.ccr.2006.09.005.
61. Bluemn, E.G., Coleman, I.M., Lucas, J.M., Coleman, R.T., Hernandez-Lopez, S., Tharakan, R., Bianchi-Frias, D., Dumpit, R.F., Kaipainen, A., Corella, A.N., et al. (2017). Androgen Receptor Pathway-Independent Prostate Cancer Is Sustained through FGF Signaling. Cancer Cell *32*, 474–489. https://doi.org/10.1016/j.ccell.2017.09.003.
62. Hanzelmann, S., Castelo, R., and Guinney, J. (2013). GSVA: gene set variation analysis for microarray and RNA-seq data. BMC Bioinf. *14*, 1–15. https://doi.org/10.1186/1471-2105-14-7.
63. de Bono, J.S., De Giorgi, U., Rodrigues, D.N., Massard, C., Bracarda, S., Font, A., Arranz Arija, J.A., Shih, K.C., Radavoi, G.D., Xu, N., et al. (2019). Randomized Phase II Study Evaluating Akt Blockade with Ipatasertib, in Combination with Abiraterone, in Patients with Metastatic Prostate Cancer with and without PTEN Loss. Clin. Cancer Res. *25*, 928–936. https://doi.org/10.1158/1078-0432.CCR-18-0981.
64. Wu, J., Wang, H., Ricketts, C.J., Yang, Y., Merino, M.J., Zhang, H., Shi, G., Gan, H., Linehan, W.M., Zhu, Y., and Ye, D. (2019). Germline mutations of renal cancer predisposition genes and clinical relevance in Chinese patients with sporadic, early-onset disease. Cancer *125*, 1060–1069. https://doi.org/10.1002/cncr.31908.
65. Lotan, T.L., Gurel, B., Sutcliffe, S., Esopi, D., Liu, W., Xu, J., Hicks, J.L., Park, B.H., Humphreys, E., Partin, A.W., et al. (2011). PTEN protein loss by immunostaining: analytic validation and prognostic indicator for a high risk surgical cohort of prostate cancer patients. Clin. Cancer Res. *17*, 6563–6573. https://doi.org/10.1158/1078-0432.CCR-11-1244.

STAR★METHODS

KEY RESOURCES TABLE

REAGENT or RESOURCE	SOURCE	IDENTIFIER
Biological samples		
FFPE embedded pre- and post-treatment samples	Fudan University Shanghai Cancer Center	N/A
Blood samples for germline DNA	Fudan University Shanghai Cancer Center	N/A
Critical commercial assays		
QIAamp DNA FFPE Advanced UNG Kit	Qiagen	https://www.qiagen.com/us/products/discovery-and-translational-research/dna-rna-purification/dna-purification/genomic-dna/qiaamp-dna-ffpe-advanced-kits
DNeasy Blood & Tissue Kit	Qiagen	https://www.qiagen.com/us/products/discovery-and-translational-research/dna-rna-purification/dna-purification/genomic-dna/dneasy-blood-and-tissue-kit
RNAstorm FFPE RNA Isolation Kit	Cell Data Sciences	https://celldatasci.com/products/RNAstorm/
Hieff NGS DNA Library Prep Kit	Yeason	https://www.yeasenbio.com/products/12927
Deposited data		
Raw sequence data	This study	GSA-Human:HRA008404
Software and algorithms		
RStudio	RStudio Inc.	https://www.rstudio.com/
R software v4.3.1	R Foundation for Statistical Computing	https://www.r-project.org/
SAS v9.3	SAS Institute Inc.	https://www.sas.com/
ggplot2	ggplot2	https://cran.r-project.org/web/packages/ggplot2/index.html
FACETS	Shen and Seshan[45]	https://github.com/mskcc/facets
Accucopy	Fan X et al.[46]	https://github.com/polyactis/Accucopy
FastQC v0.12.1	Babraham Institute	http://www.bioinformatics.babraham.ac.uk/projects/fastqc/
BWA v0.7.12	Washington University	https://bio-bwa.sourceforge.net/
GATK v4.1.9.0	Broad Institute of MIT and Harvard	https://github.com/broadinstitute/gatk/releases
VarScan v2.3.9	Johns Hopkins University	https://varscan.sourceforge.net/
scarHRD	Sztupinszki et al.[55]	https://github.com/sztup/scarHRD

EXPERIMENTAL MODEL AND STUDY PARTICIPANT DETAILS

Study design and participants

The FAST-PC trial is an investigator-initiated, single-arm, phase II clinical trial (ChiCTR2100046198, NCT05223582). This study enrolled treatment-naive men aged 18 years or older with histologically or cytologically confirmed PCa. Patients were staged using computed tomography (CT), magnetic resonance imaging (MRI), and bone scans to identify those with National Comprehensive Cancer Network (NCCN) high-risk or very high-risk PCa,[3] with or without pelvic lymph node metastasis. Key inclusion criteria included an Eastern Cooperative Oncology Group (ECOG) performance status of 0 or 1 and administration of continuous luteinizing hormone-releasing hormone analog (LHRHa) prior to RP.

Exclusion criteria included a history of other malignancies within the past five years or prior local or systemic treatment for PCa, including RP, radiotherapy, chemotherapy, PARPis, medical castration, CYP17 inhibitors, ARSis, and immunotherapy. However, prior medical castration or abiraterone treatment for no more than one month was allowed. The comprehensive eligibility criteria are detailed in the study protocol (https://www.clinicaltrials.gov/study/NCT05223582).

This trial was conducted in compliance with the Declaration of Helsinki and Good Clinical Practice guidelines. The study protocol received approval from the Ethics Committee of the Fudan University Shanghai Cancer Center (Ethics number: 2104233-5). Informed written consent was obtained from all participants prior to their inclusion in the study.

Procedures

All participants received oral fuzuloparib 150 mg twice daily, abiraterone 1000 mg once daily, prednisone 5 mg twice daily, and LHRHa treatment every 28 days for six cycles, followed by RP. Postoperatively, patients with $\leq$ ypT2N0 disease were monitored without additional treatment, while those with ypT3-4 or ypN1 disease, or positive surgical margins, were recommended to undergo adjuvant radiotherapy plus medical castration. A mandatory 90-day safety follow-up was implemented, with subsequent contact via telephone every 12 weeks to gather data on subsequent therapies and survival status until either loss to follow-up or death. Patients underwent PSA testing six weeks postoperatively and bi-monthly thereafter. Imaging assessments were performed annually or when PSA levels reached $\geq$0.2 ng/mL.

Tumor response was assessed by measuring PSA levels at each treatment cycle. Upon completion of the neoadjuvant therapy, preoperative evaluations included PSA testing and contrast-enhanced CT or MRI. An independent radiologist (B.Z.), blinded to clinical information, conducted central reviews. Post-surgery, the prostate specimens were processed into whole-mount sections, serially sectioned into 2–3 mm thick axial slices, embedded in paraffin, and a single 5-μm slice from each section was stained with hematoxylin and eosin. Central reviews of the pathological response, surgical margins, and pathologic stage were conducted by two independent pathologists (H.G., X.C.), also blinded to clinical information. The tissues deemed to be pCR or MRD were subjected to confirmatory immunohistochemistry (IHC) using AE1/AE3 and p63.

Safety evaluations included laboratory assessments, vital signs, physical examinations, 12-lead electrocardiograms, ECOG performance status, and tracking of dose interruptions, reductions, and terminations due to treatment-related adverse events (TRAEs). TRAEs and perioperative complications were monitored using the National Cancer Institute Common Terminology Criteria for Adverse Events (NCI CTCAE, version 5.0)[40] and the Clavien–Dindo Classification of Surgical Classifications,[41] respectively.

Outcomes

The primary endpoint of this study was the pathological response in the intention-to-treat (ITT) population, defined as either pCR or MRD. pCR was characterized by the absence of morphologically identifiable carcinoma in the RP specimen, while MRD was defined as a residual tumor with a maximum diameter of $\leq$5 mm in the RP specimen.

Secondary endpoints included biochemical responses, surgical margins, pathological stage, radiological responses, biochemical progression-free survival (bPFS), metastasis-free survival (MFS), and safety. bPFS was defined as the interval from RP to either a confirmed PSA level of $\geq$0.2 ng/mL or death from any cause. MFS was defined as the time from RP to investigator-assessed metastasis via prostate-specific membrane antigen positron emission tomography/computed tomography (PSMA PET/CT) imaging or death from any cause.

METHOD DETAILS

Exploratory analyses

Pre- and post-treatment tissue samples were collected via diagnostic biopsy and RP for whole-exome sequencing (WES), RNA sequencing (RNA-seq), and IHC, with both DNA and RNA extracted from FFPE tissues (Figure S11A). To address the heterogeneity inherent in PCa and its impact on biomarker research,[7,42–44] pooling multicore sequencing was performed on biopsy tissues from each patient, utilizing three to four core biopsies per patient. Post-treatment tissues underwent whole-mount pathological evaluation following RP. Experienced pathologists delineated residual tumor areas, which were then subjected to macrodissection prior to sequencing. Pre- and post-treatment samples that met sequencing quality control criteria are illustrated in Figure S11B.

DNA and RNA extraction

Genomic DNA was isolated from formalin-fixed paraffin-embedded (FFPE) tumor samples after pathologically verification to select tumor-rich sections. DNA was isolated from tumor tissue using the QIAamp DNA FFPE Advanced UNG Kit (Qiagen). DNA from whole blood was isolated using the DNeasy Blood & Tissue Kit (Qiagen) according to the manufacturer's protocol. The quantity of extracted genomic DNA was assessed by a fluorometric method with a Qubit device. RNA was extracted using the RNAstorm FFPE RNA Isolation Kit (Cell Data Sciences).

Whole-exome sequencing

Two hundred nanograms of genomic DNA was used for library preparation, using the Hieff NGS DNA Library Prep Kit (Yeason). The totality of the enriched library was used in the hybridization and captured with Twist Exome 2.0 (Twist) baits. After hybridization, the captured libraries were purified according to the manufacturer's recommendations and amplified by polymerase chain reaction. Normalized libraries were pooled, and DNA was sequenced on the Illumina sequencing platform (Nova) using a 150 bp paired-end run. The average coverage depth was 155× for whole blood control samples and 249× for tumor tissues. Finally, we utilized both FACETS[45] and Accucopy[46] to determine tumor purity and excluded samples with tumor purity <20% by both algorithms.

Variant calling

The quality of the raw reads was checked by FastQC (v0.12.1), and the low-quality reads and adapter sequences were removed by fastp (v0.23.4). Next, high-quality reads were aligned with the human reference genome GRCh38 using the Burrows–Wheeler aligner (BWA v0.7.12). After the alignment, PCR duplicates were marked using SAMBLASTER (v0.1.26). GATK base quality score recalibration was completed on the aligned BAM files (GATK v4.1.9.0) to improve the accuracy of base quality scores prior to variant calling. The germline mutations were called individually for normal samples with HaplotypeCaller (provided with GATK v4.1.9.0). Somatic single-nucleotide variants (SNVs) were identified using a validated pipeline that integrated mutation calls from different mutation callers. SNVs were called with Mutect2 (GATK v4.1.9.0) and MuSE (v1.0), and insertion/deletions (indels) were called with VarScan (v2.3.9) and Strelka (v2.9.10).

Pathogenicity for mutations

Candidate variants identified in germline DNA were determined as the valid germline variants for further analysis if they met the following criteria: (1) the allele frequency (AF) was beyond 40%; (2) supporting reads of the allele and variant were at least 15 and 8, respectively; (3) the frequency of the variants was below 1% in the public single-nucleotide polymorphism databases, including 1000 genomes (https://www.1000genomes.org/), ESP6500 (https://evs.gs.washington.edu/), ExAC (http://exac.broadinstitute.org/) and gnomAD (https://gnomad.broadinstitute.org/); (4) the variants were not synonymous SNV; (5) the variants were in the exon or splicing site.

Truncating variants (frameshift insertions/deletions, splice site mutations within 2bp of an exon-intron junction, and stopgain mutations) were presumed deleterious if they were not reported as benign or likely benign in the ClinVar database.[47] Missense mutations and non-frameshift insertions/deletions were presumed deleterious if they were reported as pathogenic or likely pathogenic in the ClinVar database[47] or defined as pathogenic or likely pathogenic by InterVar.[48] Only germline variants classified as pathogenic or likely pathogenic were further analyzed in this study.

The variants identified in tumor tissue sample were defined as the valid somatic variants if they met the following standard: (1) AF was at least 1%; (2) AF was three times higher than the AF of the same variant identified in the matched gDNA; (3) supporting reads of the allele and variant for tumor DNA were at least 15 and 8, respectively; (4) the frequency of the variant was below 1% in the public germline variants datasets, including 1000 genomes, ESP6500, ExAC and gnomAD; (5) the variant was not synonymous SNV and was in the exon or splicing site.

Pathogenic somatic mutations were identified by the following process: (1) Truncating variants (frameshift insertions/deletions, splice site mutations within 2bp of an exon-intron junction, and stopgain mutations) were presumed deleterious if they were not reported as benign or likely benign in the ClinVar database.[47] (2) Variants reported as oncogenic or likely oncogenic in OncoKB were retained and neutral variants were filtered[49]; (3) Variants of uncertain significance were further called with ClinVar[47] and InterVar.[48] Variants characterized as pathogenic or likely pathogenic were retained and variants characterized as benign or likely benign were removed. (4) Remaining variants with uncertain significance were further defined with COSMIC annotations (https://cancer.sanger.ac.uk/cosmic). The variant defined as a recurrent mutation according to COSMIC database ($\geq$3 samples with a missense substitution in the same codon, $\geq$3 samples with an inframe indel in the same codon or >10 samples with a mutation causing premature protein termination) was considered pathogenic. All other variants were classified as variants of uncertain significance. The analysis herein only included mutations screened as pathogenic.

In this study, the oncoplot displays key genes previously reported in the literatures to be associated with prostate cancer (*SPOP, MYC, PTEN, RB1, TP53*), HRR pathway (*BRCA1, BRCA2, FANCA, PALB2, CHEK2, BRIP1, ATM, CDK12, BARD1, NBN, RAD51, RAD51B, RAD51C, RAD51D, RAD54L, ATR, CHEK1, FANCL*) and AR pathway (*AR, FOXA1, NCOR1, NCOR2, SPEN*).[50–54] The HRR pathway genes were selected by taking the union of prior clinical trials involving PARPi, including GALAHAD, TRITON2, TALAPRO-2, PROPEL, and MAGNITUDE. Only variants classified as pathogenic or likely pathogenic were further analyzed in this study.

CHIP definition

CHIP variants were predefined as nonsynonymous somatic alterations (VAF $\leq$40%) in 49 genes most frequently altered in myeloid malignancies[21](ASXL1, ASXL2, BCOR, BCORL1, BRAF, CALR, CBL, CBLB, CBLC, CEBPA, CREBBP, CSF3R, CUX1, DNMT3A, EP300, ETV6, EZH2, FLT3, GATA1, GATA2, GNB1, IDH1, IDH2, JAK2, KDM6A, KIT, KMT2A, KRAS, MPL, NF1, NPM1, NRAS, PPM1D, PRPF8, PTEN, PTPN11, RAD21, RUNX1, SETBP1, SF3B1, SMC1A, SMC3, SRSF2, STAG2, TET2, TP53, U2AF1, WT1, ZRSR2).

Copy number evaluation

Copy number variants (CNVs) were assessed with CNVkit (v0.9.8) in the aligned sequencing reads. Significantly amplified or deleted regions of copy number variants were identified by GISTIC (v.2.0.23). Log2 copy-number ratio cutoffs to define deep deletions, shallow deletions, gains, and amplifications, respectively were < -1, -1 to -0.3, 0.3 to 1, and >1. Amplification/gain in oncogenes and deep deletion/shallow deletion in tumor suppressor genes (TSGs) are considered pathogenic.

HRR allelic

We considered "biallelic" events those cases with either: (1) two pathogenic mutations; (2) a pathogenic mutation and a shallow deletion; (3) a pathogenic mutation and loss-of-heterozygosity; or (4) cases with homozygous deletions.

HRD score, TMB and FGA

The HRD score was obtained through the scarHRD pipeline.[55] Tumor mutational burden (TMB) was calculated as the number of non-synonymous somatic mutations per mega-base within the sequenced region. Fraction of genome altered (FGA) was defined as the size of the sequenced genome with log2 copy number variation (gain or loss) > 0.2 divided by the total size of the genome for which the copy number was profiled. For a patient with multiple lesion samples post-treatment, the average value of all lesions was used to perform paired comparisons between pre-treatment and post-treatment samples.

RNA-seq

Total RNAs were treated with DNase I (NEB) prior to the construction of RNA-seq libraries. The SMART cDNA synthesis technology (Clontech) was used to generate strand-specific RNA-seq libraries. CRISPR/Cas9 technology was employed to deplete the ribosomal and mitochondrial cDNA. The resulting purified dsDNA underwent 13 cycles of PCR amplification. Quality control was performed using Qubit (Thermo Fisher Scientific) and Qsep100 (BiOptic) before the libraries were sequenced on the Illumina sequencing platform (Nova) using a 150 bp paired-end run. The RNA-seq data sequencing reads were aligned to the reference genome (Genome Reference Consortium GRCh38) using the spliced read aligner HISAT2, which was provided with the Ensembl human genome assembly.

STAR-Fusion v1.12.013 was used to call fusions like TMPRSS2-ERG.

Differentially expressed genes and pathway enrichment analysis

Differentially expressed genes between pre- and post-treatment were analyzed using Deseq2 v1.42.1 log2(fold change) > 1 and adjusted p values <0.05 were considered the cutoff criteria for differentially expressed gene analysis.

The gene list from differential analysis was ordered by decreasing log2 fold change. Pathway enrichment was analyzed by clusterProfiler v.4.10.1, and Gene Set Enrichment Analysis (GSEA) were analyzed for their q-value, with gene signatures of cancer hallmarks[56] and Pathway Interaction Database[57] obtained from Molecular Signatures Database (www.gsea-msigdb.org/gsea/msigdb). Pathways were considered significant at Benjamin–Hochberg-adjusted q-values <0.05.

ARG10, AR signature, and NE score

The calculation of ARG10 is based on the method by Westbrook et al.[58]: TPM gene expression values were log2(TPM +1) transformed and converted to z-scores by: $z = (x - \mu)/\sigma$, where μ is the average log2(TPM +1) across all samples of a gene and σ is the standard deviation of the log2(TPM +1) across all samples of a gene. The ARG10 of each sample was the average Z score of all genes in ARG10 signature.[59] The AR signature (30 genes that were previously reported as defining the pathway[60]) and NE score (10-gene signature from Bluemn[61]) were calculated in R using GSVA v1.48.3 package with default parameters using TPM data as input.[62] For a patient with multiple lesion samples post-treatment, the average value of all lesions was used to perform paired comparisons between pre-treatment and post-treatment samples.

PCA and unsupervised clustering

To understand the overall transcriptional similarities across all the samples, Principal component analysis (PCA) and unsupervised clustering was performed using RNA-seq data. Briefly, the filtered count matrix was transformed using the vst function implemented in DESeq2 R package (v 1.42.1). The transformed values were used to compute the sample-to-sample Euclidean distance metric for hierarchical clustering through the 'complete' method. The distance matrix was used to generate heatmap using pheatmap R package (v 1.0.12).

PTEN immunohistochemistry

Formalin-fixed paraffin-embedded tumor tissue was retrieved for IHC analysis. IHC was performed using the SP218 (1:200) PTEN antibody according to previous reports. PTEN status classification was based on the tumor with the lowest PTEN staining.[63,64] Lesions were defined as PTEN loss status if they either showed a complete absence of PTEN staining or weak intensity staining compared with surrounding benign tissue or stroma in more than 50% of malignant cells with no specific cytoplasmic staining.[65] The IHC results were independently analyzed by two experienced urologic pathologists blinded to clinical data. A consensus would be reached when discrepancies occurred.

QUANTIFICATION AND STATISTICAL ANALYSIS

The sample size for this study was determined using Simon's Minimax two-stage design. The null hypothesis of a pCR/MRD of 24%[19] and an alternative hypothesis of 44% were set with a one-sided alpha of 5% and 80% power. Initially, 23 patients were to be enrolled

in the first stage, and if six or more patients achieved pCR/MRD, an additional 11 patients would be recruited in the second stage. The primary endpoint would be met if at least 13 patients achieved pCR/MRD.

Efficacy analyses were conducted in both the ITT population and the per-protocol (PP) population, which included patients who received at least one dose of the study treatment and those who completed neoadjuvant treatment and RP according to the protocol, respectively. Safety analyses were performed on the safety population, encompassing all patients who received at least one dose of the study treatment.

Statistical analyses were executed using SAS software (version 9.3) and R software (version 4.3.1). Comparisons between groups were made using Wilcoxon rank-sum test for continuous variables. The Wilcoxon signed-rank test was utilized to compare matched pre- and post-treatment samples. bPFS and MFS were estimated using the Kaplan-Meier method, with group differences assessed via the log rank test. Logistic regression and Cox proportional hazards regression models were employed to calculate odds ratios (OR) and hazard ratios (HR), respectively, for the construction of forest plots. All statistical tests were two-sided, and a p value <0.05 was considered statistically significant. p values were adjusted for multiple comparisons using the Benjamini-Hochberg procedure where applicable.

ADDITIONAL RESOURCES

This study has been registered with ClinicalTrials.gov, NCT05223582.